Hydrodynamical view of massive stars' winds

Michel Curé
Instituto de Física y Astronomía
Universidad de Valparaíso

Massive Stars Winds

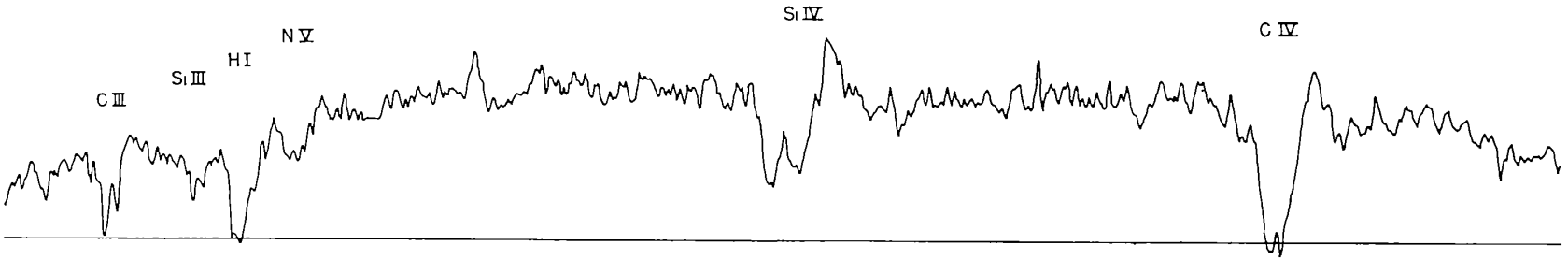

Fig. 1. Densitometer tracing, on an intensity scale, of the far-ultraviolet spectrum of ζ Orionis, photographed by Princeton on September 10, 1966. The distribution of intensity with wavelength includes the unknown response of the spectrograph. Wavelengths increase towards the right from 1140 to 1630 Å. The H I line is interstellar, but all the other identified absorption features are circumstellar with large Doppler shifts to shorter wavelengths.

Massive Stars Winds

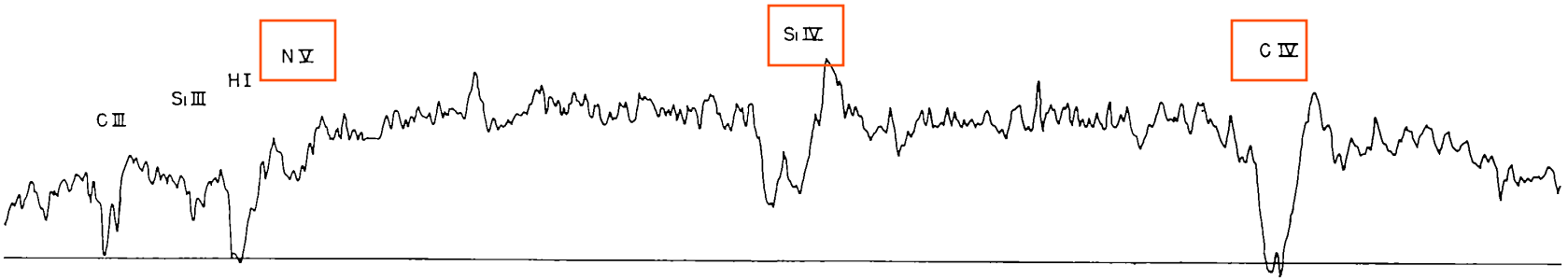

Fig. 1. Densitometer tracing, on an intensity scale, of the far-ultraviolet spectrum of ζ Orionis, photographed by Princeton on September 10, 1966. The distribution of intensity with wavelength includes the unknown response of the spectrograph. Wavelengths increase towards the right from 1140 to 1630 Å. The H I line is interstellar, but all the other identified absorption features are circumstellar with large Doppler shifts to shorter wavelengths.

Massive Stars Winds

Formation of a P-Cygni Line- Profile

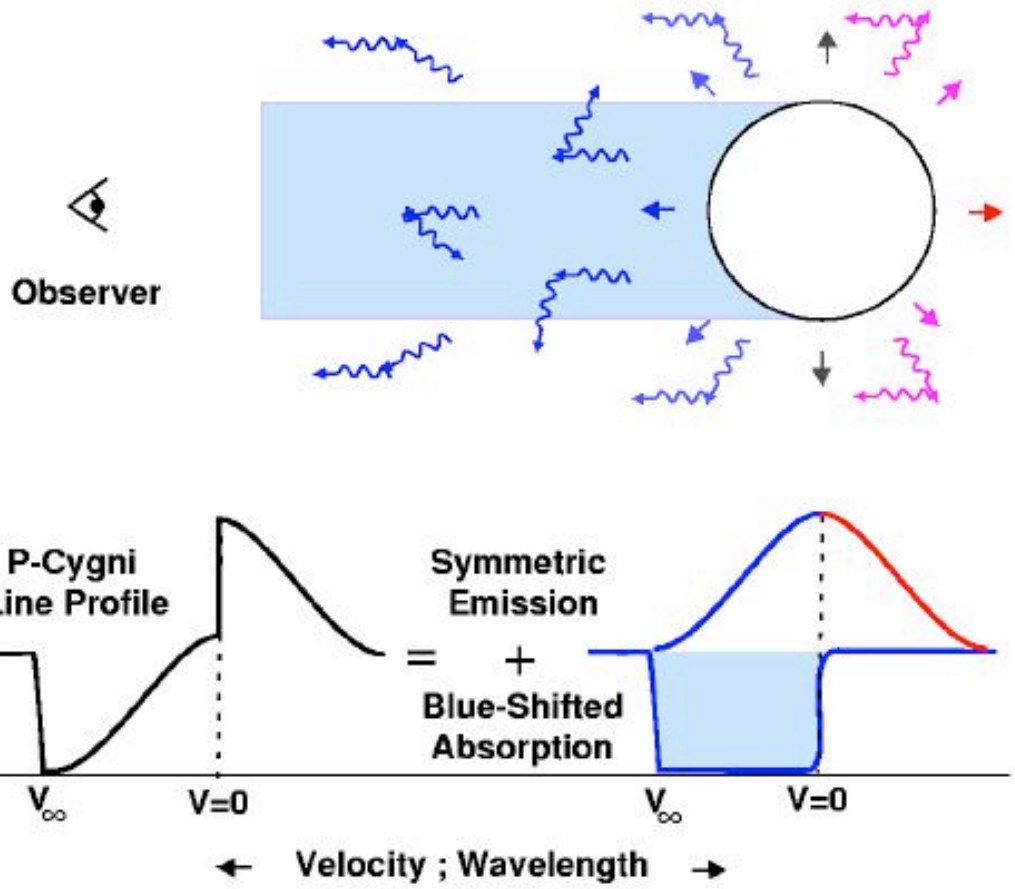

Driven Mechanism

Only known Theory in the ’60:

Parker’s Model for the Solar Wind

(Parker, E.N.: 1960, ApJ 132, 821)

For O stars => Teff = 10^7 K

But at this Temperature C IV - N V - Si IV Don’t Exist

Destroyed by collisional ionisation

Driven Mechanism

Lucy & Solomon (1970, ApJ, 159, 870):
Wind driven by resonance lines
Obtained only mass loss rates of about 1/100th of the observed values

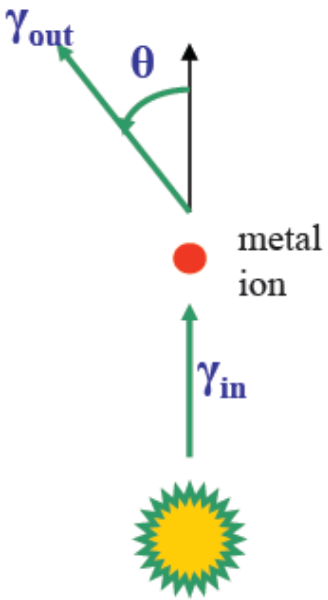

$$\cos\theta_{in} \approx 1$$

isotropic reemission

$$\langle \cos\theta_{out} \rangle = 0$$

Driven Mechanism

Castor, Abbott & Klein (1975, ApJ, 195, 157)
Wind driven by an ensemble of lines (scattering)
They obtained a qualitative agreement with observational values

Driven Mechanism

Castor, Abbott & Klein (1975, ApJ, 195, 157)
Wind driven by an ensemble of lines (scattering)
They obtained a qualitative agreement with observational values

The Standard Model (m-CAK)

Line Force

Contribution from an ensemble of lines
Currently: ~Mega lines, ~150 ionisation stages (H –Zn),

Line Force

Contribution from an ensemble of lines
Currently: ~Mega lines, ~150 ionisation stages (H –Zn),

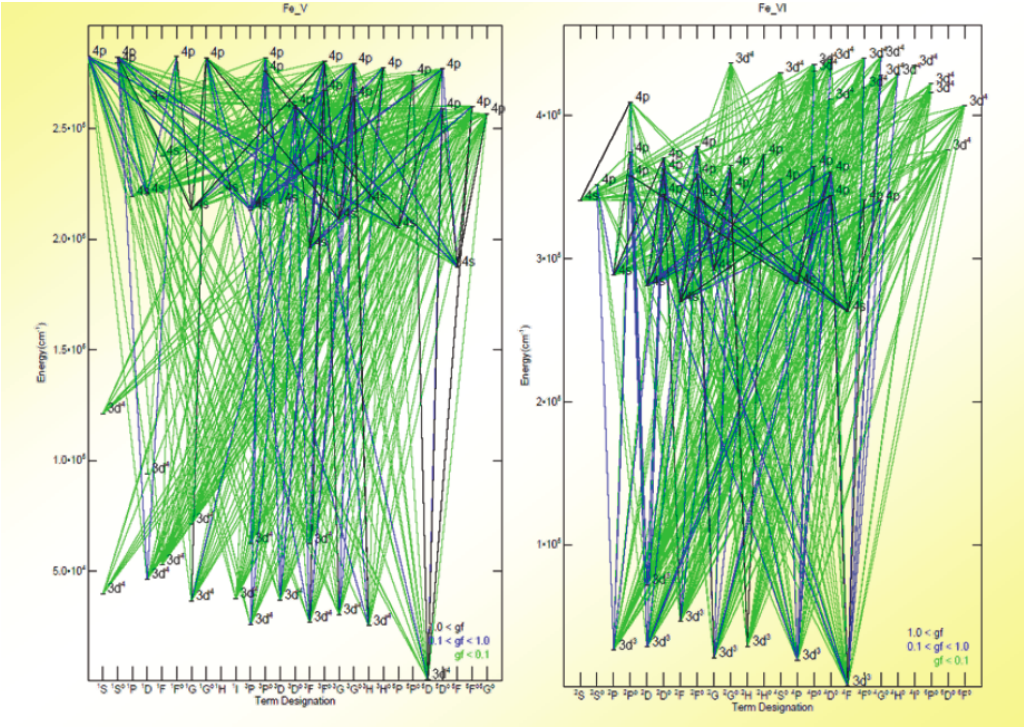

Line Force

Contribution from an ensemble of lines
Currently: ~Mega lines, ~150 ionisation stages (H –Zn),

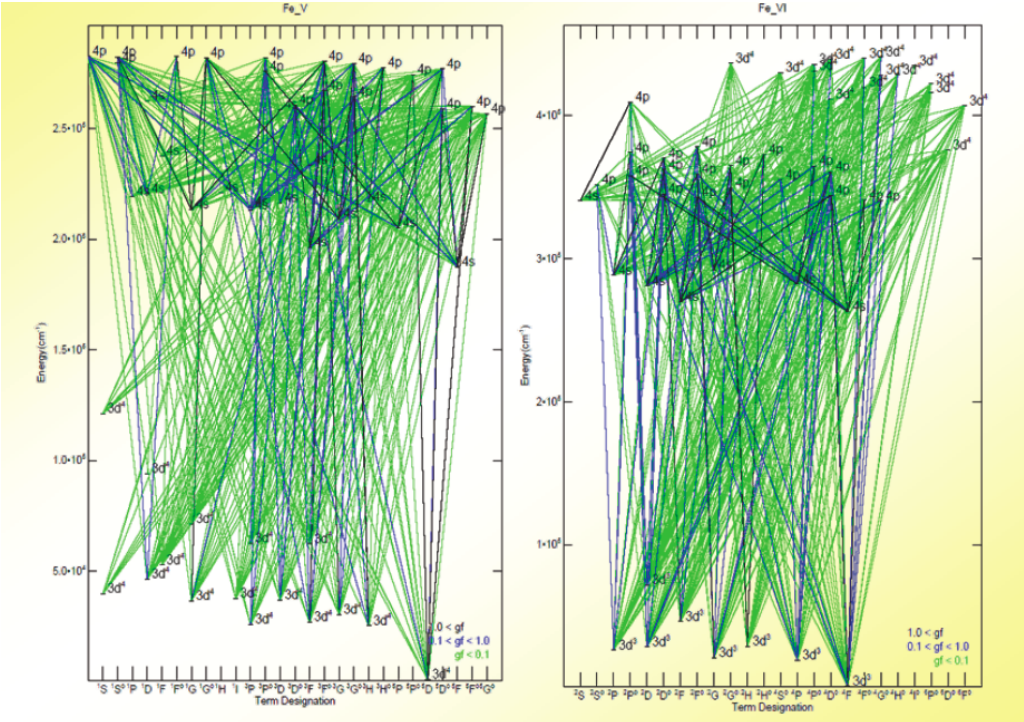

	I	II	III	IV	V	VI	VII	VIII
1	H_I							
2	He_I	He_II						
6	C_I	C_II	C_III	C_IV	C_V			
7	N_I	N_II	N_III	N_IV	N_V	N_VI		
8	O_I	O_II	O_III	O_IV	O_V	O_VI		
9	F_I	F_II	F_III	F_IV	F_V	F_VI		
10	Ne_I	Ne_II	Ne_III	Ne_IV	Ne_V	Ne_VI		
11	Na_I	Na_II	Na_III	Na_IV	Na_V	Na_VI		
12	Mg_I	Mg_II	Mg_III	Mg_IV	Mg_V	Mg_VI		
13	Al_I	Al_II	Al_III	Al_IV	Al_V	Al_VI		
14	Si_I	Si_II	Si_III	Si_IV	Si_V	Si_VI		
15	P_I	P_II	P_III	P_IV	P_V	P_VI		
16	S_I	S_II	S_III	S_IV	S_V	S_VI	S_VII	
17	Cl_I	Cl_II	Cl_III	Cl_IV	Cl_V	Cl_VI		
18	Ar_I	Ar_II	Ar_III	Ar_IV	Ar_V	Ar_VI	Ar_VII	ArVIII
19	K_I	K_II	K_III	K_IV	K_V	K_VI		
20	Ca_I	Ca_II	Ca_III	Ca_IV	Ca_V	Ca_VI		
22	Ti_I	Ti_II	Ti_III	Ti_IV	Ti_V			
23	V_I	V_II	V_III	V_IV	V_V			
24	Cr_I	Cr_II	Cr_III	Cr_IV	Cr_V	Cr_VI		
25	Mn_I	Mn_II	Mn_III	Mn_IV	Mn_V	Mn_VI		
26	Fe_I	Fe_II	Fe_III	Fe_IV	Fe_V	Fe_VI	Fe_VII	FeVIII
27	Co_I	Co_II	Co_III	Co_IV	Co_V	Co_VI	Co_VII	
28	Ni_I	Ni_II	Ni_III	Ni_IV	Ni_V	Ni_VI	Ni_VII	NiVIII
29	Cu_I	Cu_II	Cu_III	Cu_IV	Cu_V	Cu_VI		
30	Zn_I	Zn_II	Zn_III					

atomic data status:

excellent	good	poor	bad

Assumptions

Stationary - Low viscosity - Spherical symmetry - No Mag. Fields.

Mass Conservation

$$\dot{M} = 4\,\pi\, r^2\, \rho\, v$$

Momentum Conservation

$$v\,\frac{dv}{dr} = -\frac{1}{\rho}\,\frac{dP}{dr} - \frac{G\,M\,(1-\Gamma)}{r^2} + g^{line}\left(\rho, \frac{dv}{dr}, n_e\right)$$

Inertia — Gas Pressure — Gravity — Line Force

Michel Curé
Universidad de Valparaíso

Radiation Driven Winds

Michel Curé
Universidad de Valparaíso

Radiation Driven Winds

$$g^{line} = \frac{C(k,\dot{M})}{r^2} CF\left(r, v, \frac{dv}{dr}\right) \left(r^2 v \frac{dv}{dr}\right)^{\alpha} \left(\frac{n_e}{W(r)}\right)^{\delta}$$

Michel Curé
Universidad de Valparaíso

Radiation Driven Winds

Eigenvalue

$$g^{line} = \frac{C(k,\dot{M})}{r^2} CF\left(r, v, \frac{dv}{dr}\right) \left(r^2 v \frac{dv}{dr}\right)^{\alpha} \left(\frac{n_e}{W(r)}\right)^{\delta}$$

Radiation Driven Winds

Eigenvalue

$$g^{line} = \frac{C(k,\dot{M})}{r^2} CF\left(r, v, \frac{dv}{dr}\right) \left(r^2 v \frac{dv}{dr}\right)^{\alpha} \left(\frac{n_e}{W(r)}\right)^{\delta}$$

Finite Disk
Correction Factor

Radiation Driven Winds

Ensemble of lines

Eigenvalue

$$g^{line} = \frac{C(k,\dot{M})}{r^2} CF\left(r, v, \frac{dv}{dr}\right) \left(r^2 v \frac{dv}{dr}\right)^{\alpha} \left(\frac{n_e}{W(r)}\right)^{\delta}$$

Finite Disk
Correction Factor

Michel Curé
Universidad de Valparaíso

Radiation Driven Winds

Ensemble of lines

Eigenvalue

$$g^{line} = \frac{C(k,\dot{M})}{r^2} CF\left(r, v, \frac{dv}{dr}\right) \left(r^2 v \frac{dv}{dr}\right)^{\alpha} \left(\frac{n_e}{W(r)}\right)^{\delta}$$

Finite Disk
Correction Factor

Changes in
Ionisation

Michel Curé
Universidad de Valparaíso

Radiation Driven Winds

Ensemble of lines

Eigenvalue

$$g^{line} = \frac{C(k,\dot{M})}{r^2} CF\left(r, v, \frac{dv}{dr}\right) \left(r^2 v \frac{dv}{dr}\right)^{\alpha} \left(\frac{n_e}{W(r)}\right)^{\delta}$$

Finite Disk
Correction Factor

Changes in
Ionisation

Michel Curé
Universidad de Valparaíso

Change of variables

$$u = \frac{-R_*}{r},$$
$$w = \frac{v}{a},$$
$$w' = \frac{dw}{du},$$

Equation of Motion

$$F(u, w, w') = 0$$

$$F(u, w, w') \equiv \left(1 - \frac{1}{w^2}\right) w \frac{dw}{du} + A + \frac{2}{u} + a_{\rm rot}^2 u - C' C F g(u) (w)^{-\delta} \left(w \frac{dw}{du}\right)^{\alpha} = 0$$

Non-Rotating Solution Schema

Non-Rotating Solution Schema

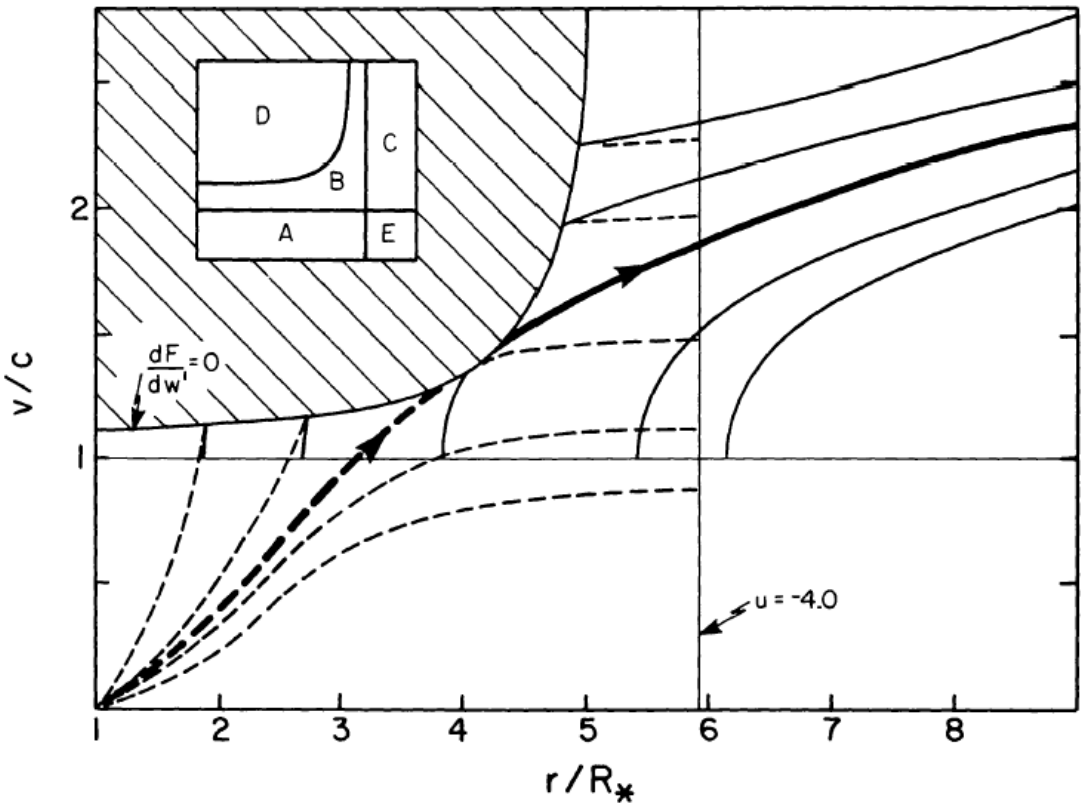

Michel Curé
Universidad de Valparaíso

Non-Rotating Solution Schema

Singularity Condition

$$\frac{\partial F(u, w, w')}{\partial w'} = 0$$

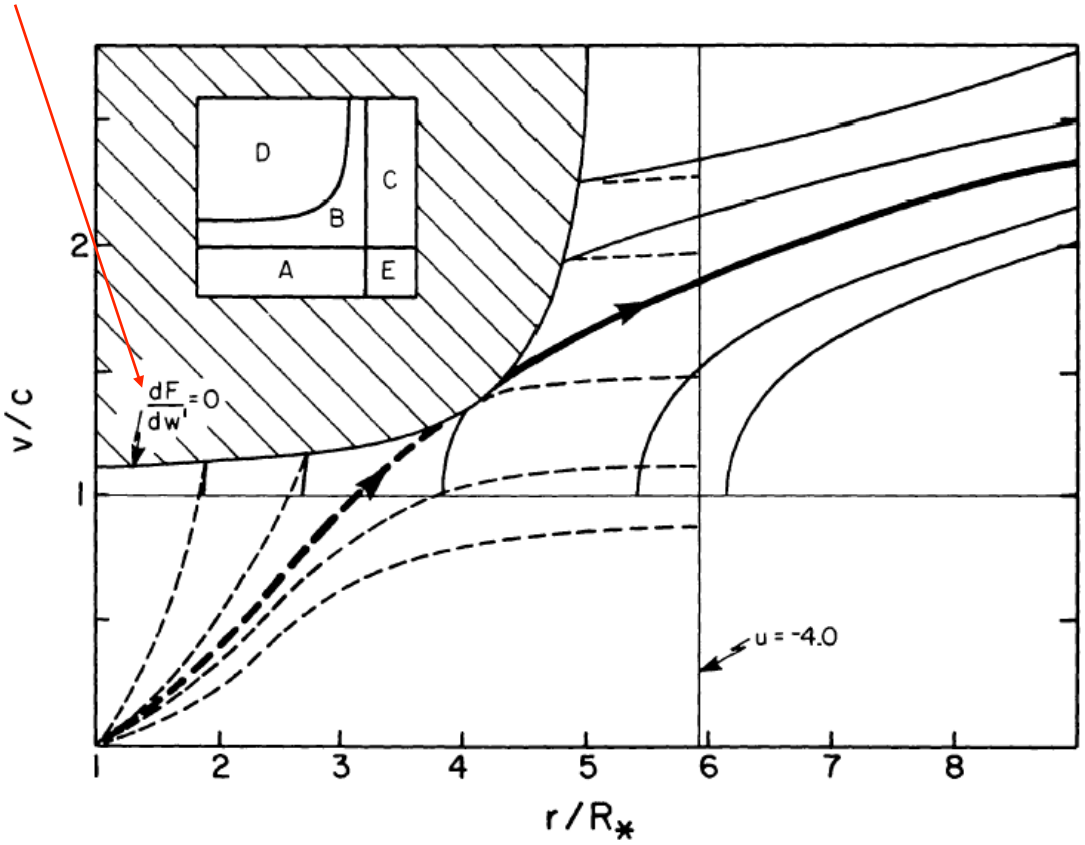

Michel Curé
Universidad de Valparaíso

Non-Rotating Solution Schema

Singularity Condition

$$\frac{\partial F(u, w, w')}{\partial w'} = 0$$

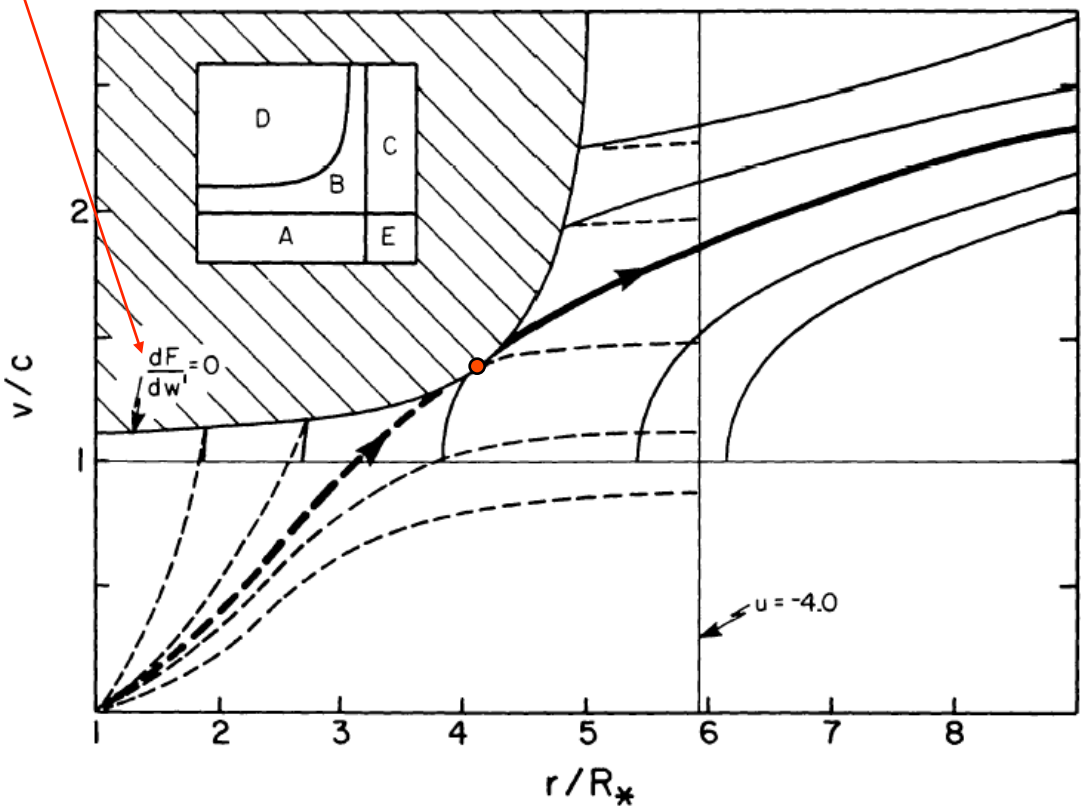

Michel Curé
Universidad de Valparaíso

First Topological Analysis

Non-Rotating Solution Schema

Singularity Condition

$$\frac{\partial F(u,w,w')}{\partial w'} = 0$$

Regularity Condition

$$\frac{dF(u,w,w')}{du} = \frac{\partial F}{\partial u} + \frac{\partial F}{\partial w} w' = 0$$

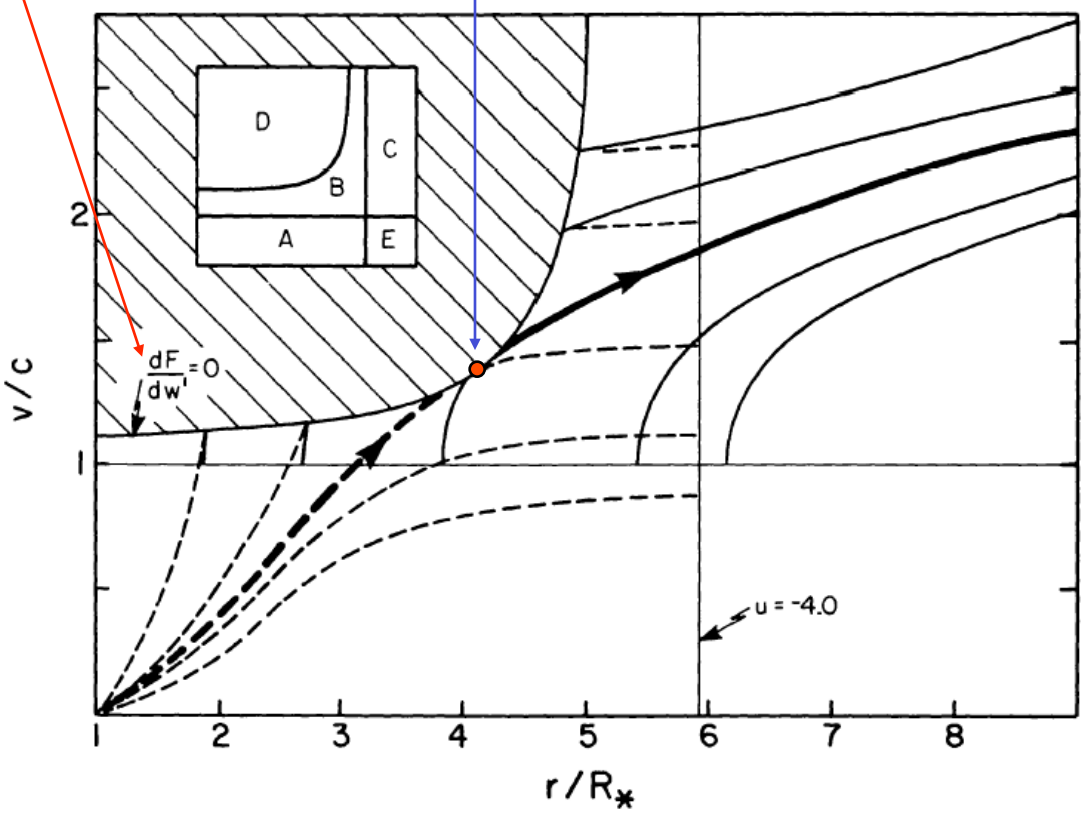

Michel Curé
Universidad de Valparaíso

m-CAK Model

modified-CAK Theory:
Finite Disk Correction Factor

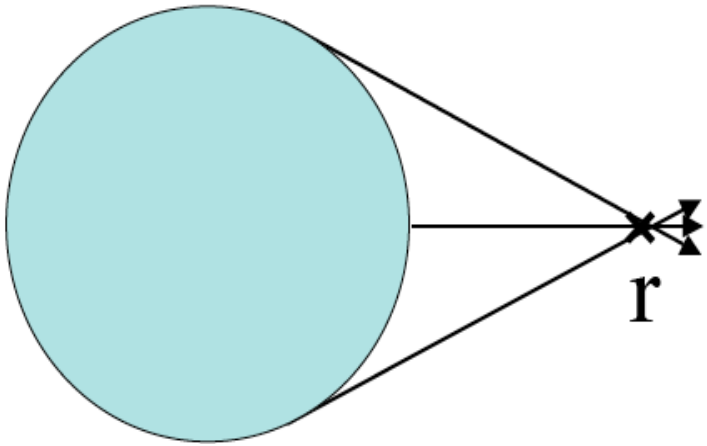

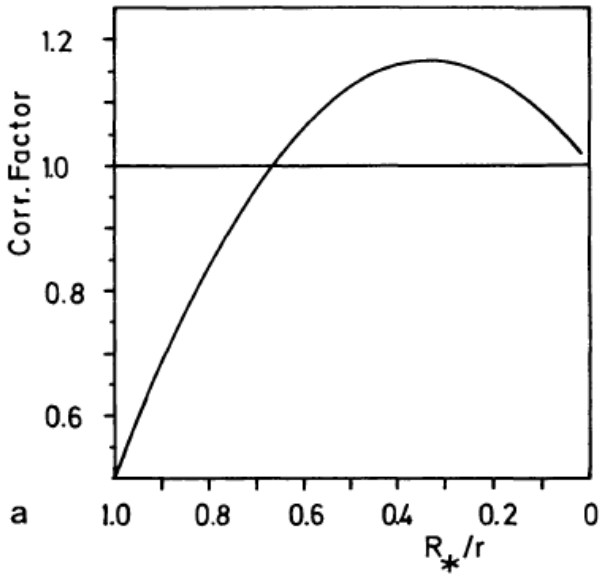

Friend & Abbott
ApJ, 311,701,1986

Pauldrach, Puls & Kudritzki
A&A, 164,86, 1986

Michel Curé
Universidad de Valparaíso

m-CAK Model

m-CAK: better agreement with observations

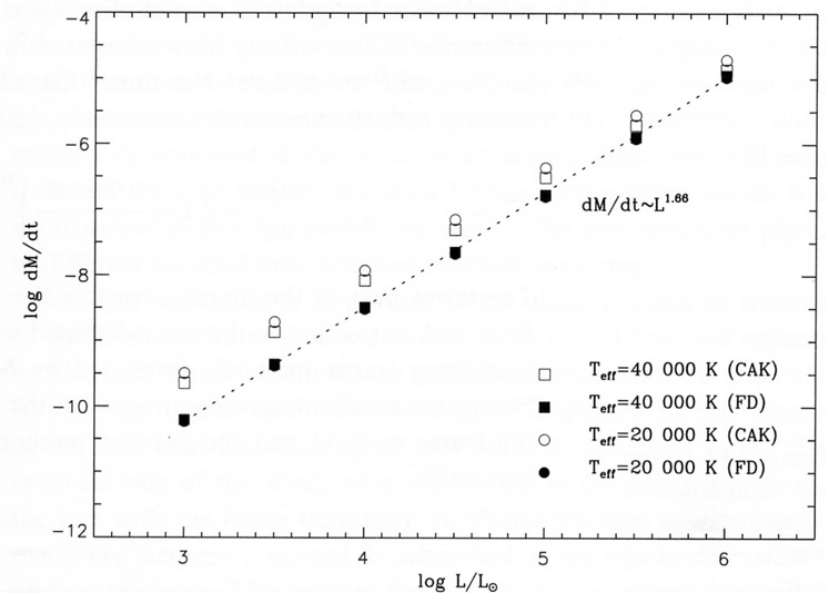

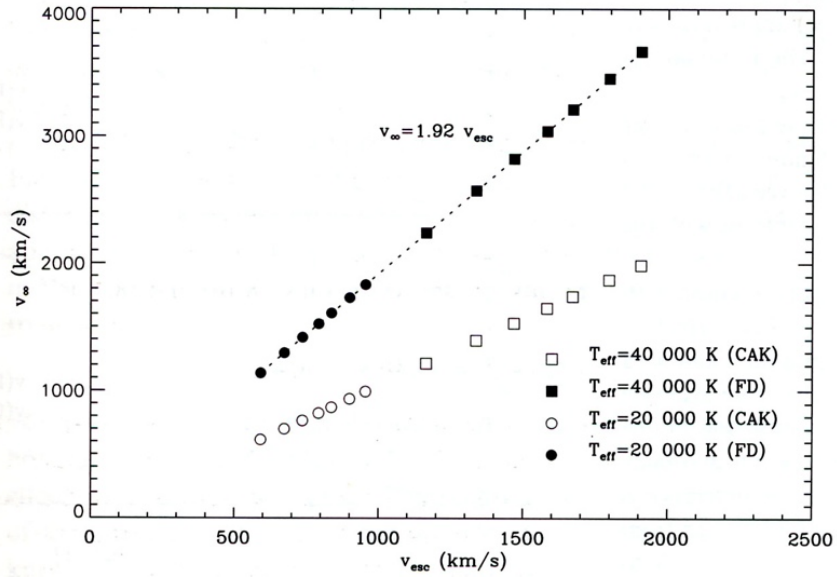

The β Law

$$v(r) = v_\infty \, (1 - R_*/r)^\beta$$

Michel Curé
Universidad de Valparaíso

Slow solutions

Ω-Slow Solution

The Astrophysical Journal, 614:929–941, 2004 October 20

THE INFLUENCE OF ROTATION IN RADIATION-DRIVEN WIND FROM HOT STARS: NEW SOLUTIONS AND DISK FORMATION IN Be STARS

Michel Curé
Departamento de Física y Meteorología, Universidad de Valparaíso, Casilla 5030, Valparaíso, Chile; michel.cure@uv.cl
Received 1999 December 28; accepted 2004 June 18

ABSTRACT

The theory of radiation-driven wind including stellar rotation is reexamined. After a suitable change of variables, a new equation for the mass-loss rate is derived analytically. The solution of this equation remains within 1% confidence when compared with numerical solutions. In addition, a nonlinear equation for the position of the critical (singular) point is obtained. This equation shows the existence of an additional critical point besides the standard m-CAK critical point. For a stellar rotation velocity larger than ~ 0.7–$0.8 V_{\rm bkup}$, there exists only one critical point, located away from the star's surface. Numerical solutions crossing through this new critical point are attained. In these cases, the wind has a very low terminal velocity and therefore a higher density. Disk formation in Be stars is discussed in the framework of this new line-driven stellar wind solution.

Subject headings: hydrodynamics — methods: analytical — stars: early-type — stars: mass loss — stars: rotation — stars: winds, outflows

Ω-Slow Solution

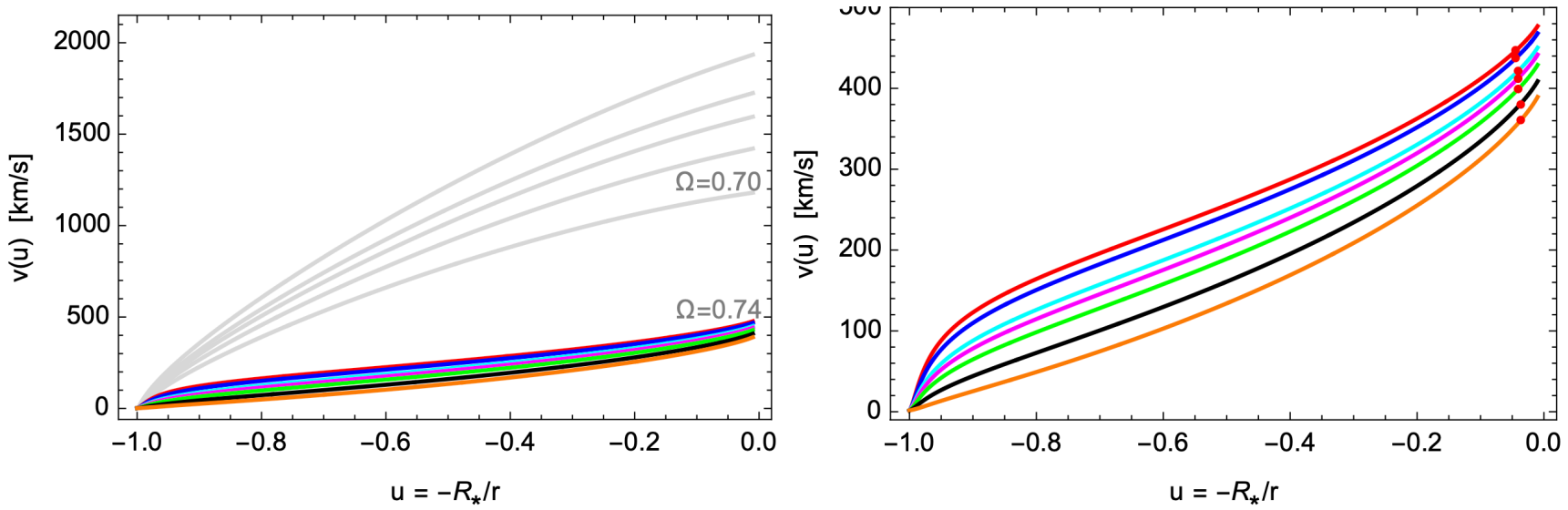

Figure 8. Velocity profiles, $v(u)$, as function of the rotational rate Ω. Left panel: fast solutions ($\Omega \lesssim 0.74$) are plotted in grey lines, while the Ω-slow solutions are in coloured lines: $\Omega = 0.74$ (red line), $\Omega = 0.76$ (blue line), $\Omega = 0.80$ (cyan line), $\Omega = 0.82$ (magenta line), $\Omega = 0.85$ (green line), $\Omega = 0.90$ (black line), and $\Omega = 0.95$ (orange line). Right panel: The same Ω-slow solutions, but zoomed and including the location of the singular points (red dots).

δ-Slow Solution

The Astrophysical Journal, 737:18 (5pp), 2011 August 10 doi:10.1088/0004-637X/737/1/18

SLOW RADIATION-DRIVEN WIND SOLUTIONS OF A-TYPE SUPERGIANTS

M. Curé[1], L. Cidale[2,4], and A. Granada[2,3]
[1] Departamento de Física y Astronomía, Facultad de Ciencias, Universidad de Valparaíso Av. Gran Bretaña 1111, Casilla 5030, Valparaíso, Chile; michel.cure@uv.cl
[2] Departamento de Espectroscopía, Facultad de Ciencias Astronómicas y Geofísicas, Universidad Nacional de La Plata (UNLP), and Instituto de Astrofísica La Plata, CCT La Plata, CONICET-UNLP Paseo del Bosque S/N, 1900 La Plata, Argentina
[3] Observatoire Astronomique de l'Université de Genève 51, Chemin des Maillettes, CH-1290, Sauverny, Switzerland
Received 2011 February 24; accepted 2011 May 20; published 2011 July 25

δ-Slow Solution

To present the topological analysis of this type of solution, we adopt the model T19 from Venero et al. [53]. The stellar and line-force parameters are $T_{\rm eff} = 19000K$, $\log g = 2.5$, $R/R_\odot = 40$, $k = 0.32$, and $\alpha = 0.5$. We use $\tau_* = 2/3$ as a boundary condition at the stellar surface.

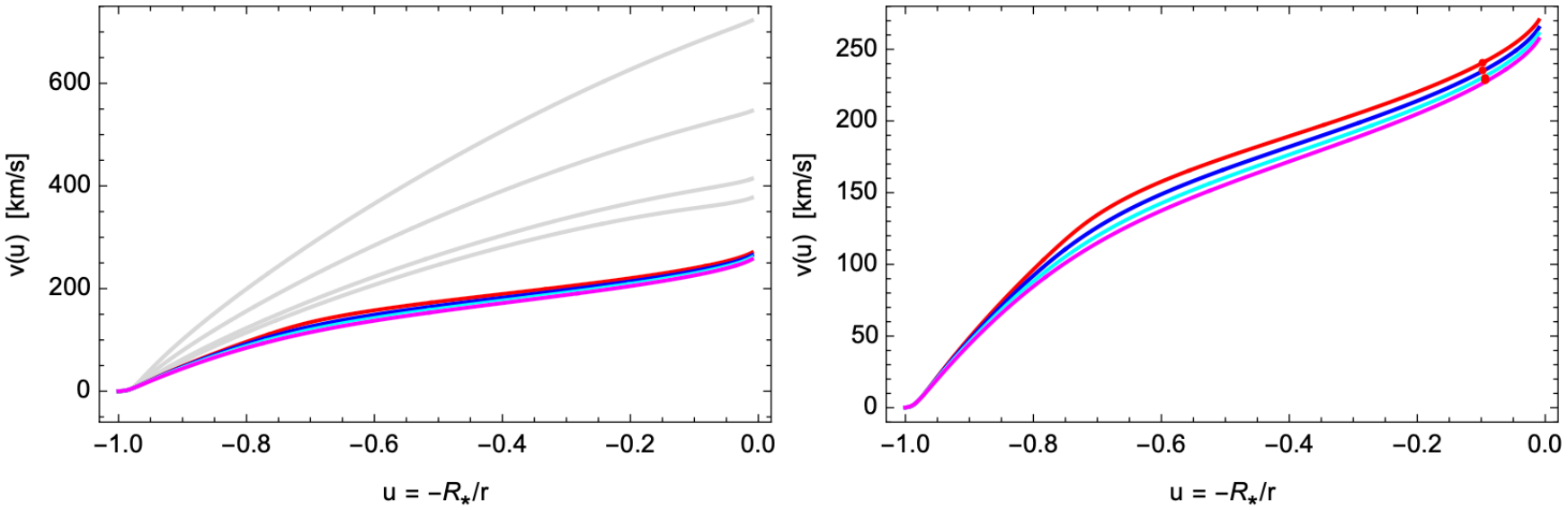

Figure 11. Velocity profiles, $v(u)$, for different values of the line-force parameter δ. Left panel: fast solutions are plotted in grey lines for $\delta = 0.0, 0.1, 0.2, 0.24$, while δ-slow solutions are in coloured lines. Red line corresponds to $\delta = 0.3$, blue line to $\delta = 0.31$, cyan line to $\delta = 0.32$, and magenta line to $\delta = 0.33$. The right panel shows only δ-slow solutions, and the location of the singular points for each solution is shown with a red dot.

Detailed CAK topological analysis

A&A 428, 545–554 (2004)
DOI: 10.1051/0004-6361:20040325

Astronomy & Astrophysics

The influence of rotation in radiation driven winds from hot stars

II. CAK topological analysis

M. Curé[1] and D. F. Rial[2]

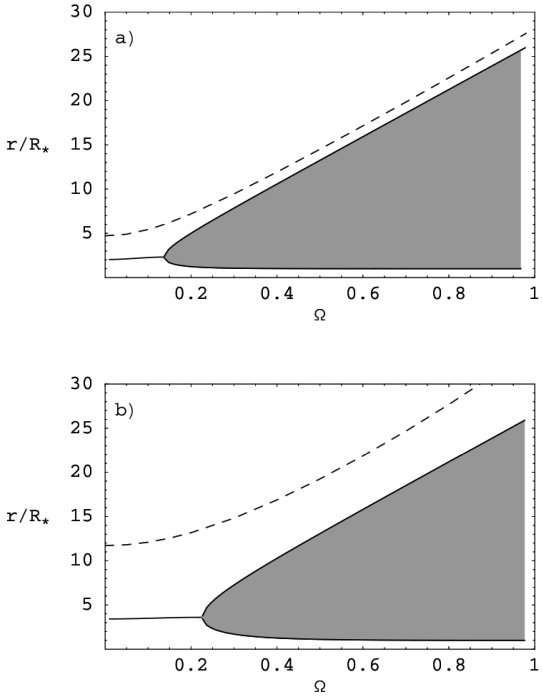

Fig. 6. The curves $r_{\min}$ and $r_{\pm}$ are shown with continuous lines as function of Ω. These curves represent the boundaries for the type of the singular point topology. The numerical results for the location of the singular point is also shown in dashed-line. **a)** is for $\delta = 0.02$ and **b)** for $\delta = 0.1$. See text for details.

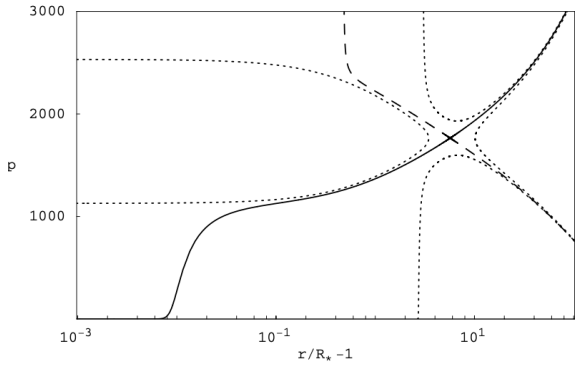

Fig. 7. The topology of the rotating-CAK model, p versus $r/R_* - 1$ for $\Omega = 0.25$ and $\delta = 0.02$. The unique curve that starting at the stellar surface and reaches infinity is the CAK original solution (continuous-line).

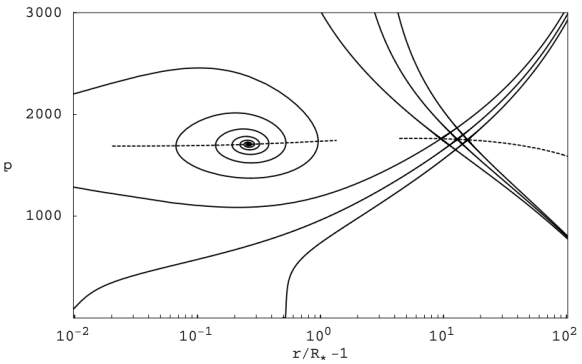

Detailed m-CAK topological analysis

Astron. Nachr. / AN **328**, No. 6, 513 – 520 (2007) / **DOI** 10.1002/asna.200610748

A new numerical method for solving radiation driven winds from hot stars

M. Curé[1,⋆] and **D.F. Rial**[2,1]

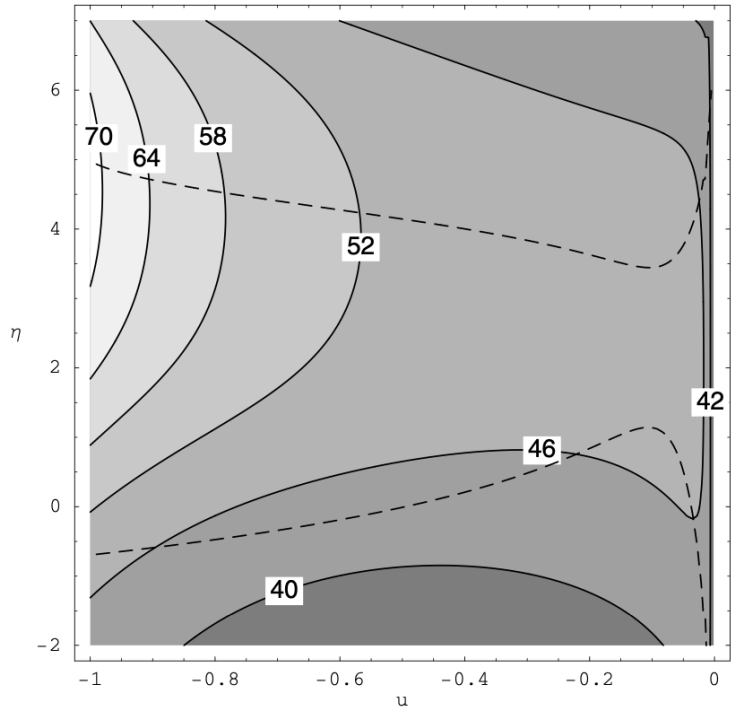

Fig. 1 The iso-contours $R(u,\eta) = 0$ (dashed line) and iso-contours $H(u,\eta,\bar{C}) = 0$ (solid-lines) for different labelled values of $\bar{C}$ as function of the variables u and η. See text for details.

Table 3 Singular points coordinates.

Label	$\bar{C}$	r_c	u_c	η_c	ζ_c
A	70	1.018	−0.982	+4.905	+7.468
B	46	1.116	−0.896	−0.587	+5.638
C	46	4.505	−0.222	+0.753	+7.253
D	46	29.41	−0.034	−0.176	+7.344
E	46	40.32	−0.020	+4.605	+7.439

	$\det(B)$	Topology
A	−	X-type
B	−	X-type
C	+	Spiral
D	−	X-type
E	−	X-type

Detailed m-CAK topological analysis

Astron. Nachr. / AN **328**, No. 6, 513 – 520 (2007) / **DOI** 10.1002/asna.200610748

A new numerical method for solving radiation driven winds from hot stars

M. Curé[1,⋆] and **D.F. Rial**[2,1]

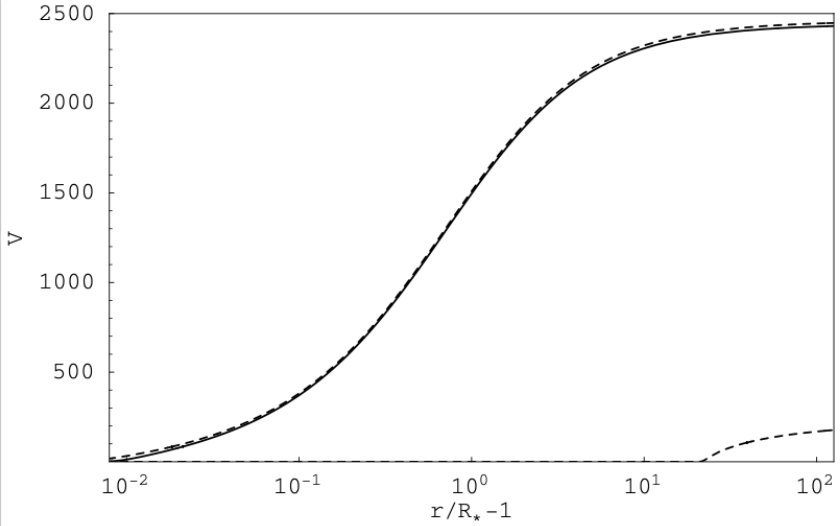

Fig. 2 Velocity (in km s^{-1}) versus $(r/R_* - 1)$. The unique curve that starts at the stellar surface and reaches infinity is the m-CAK original solution (solid line). See text for details.

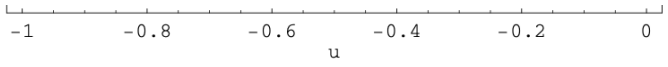

Fig. 1 The iso-contours $R(u,\eta) = 0$ (dashed line) and iso-contours $H(u,\eta,\bar{C}) = 0$ (solid-lines) for different labelled values of $\bar{C}$ as function of the variables u and η. See text for details.

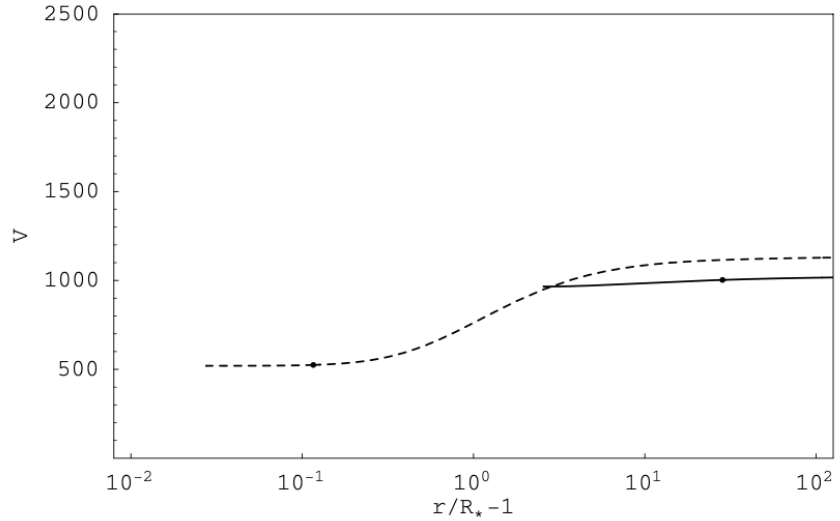

Fig. 3 Velocity (in km s^{-1}) versus $(r/R_* - 1)$. The solution that passes through singular point B (dashed-line) reaches the photosphere with a too high value of the velocity. While the solution passing through the singular point D (solid-line) does not reach the photosphere. See text for details.

D	–	X-type
E	–	X-type

galaxies

MDPI

Review

Radiation-Driven Wind Hydrodynamics of Massive Stars: A Review

Michel Curé [1,*] and Ignacio Araya [2]

[1] Instituto de Física y Astronomía, Universidad de Valparaíso, Gran Bretaña 1111, Valparaíso 2340000, Chile
[2] Vicerrectoría de Investigación, Universidad Mayor, Santiago 8580745, Chile; ignacio.araya@umayor.cl
* Correspondence: michel.cure@uv.cl

Wind Solutions

Spherical solutions

Fast and δ-Slow Wind Solutions

Quantitative Spectroscopy

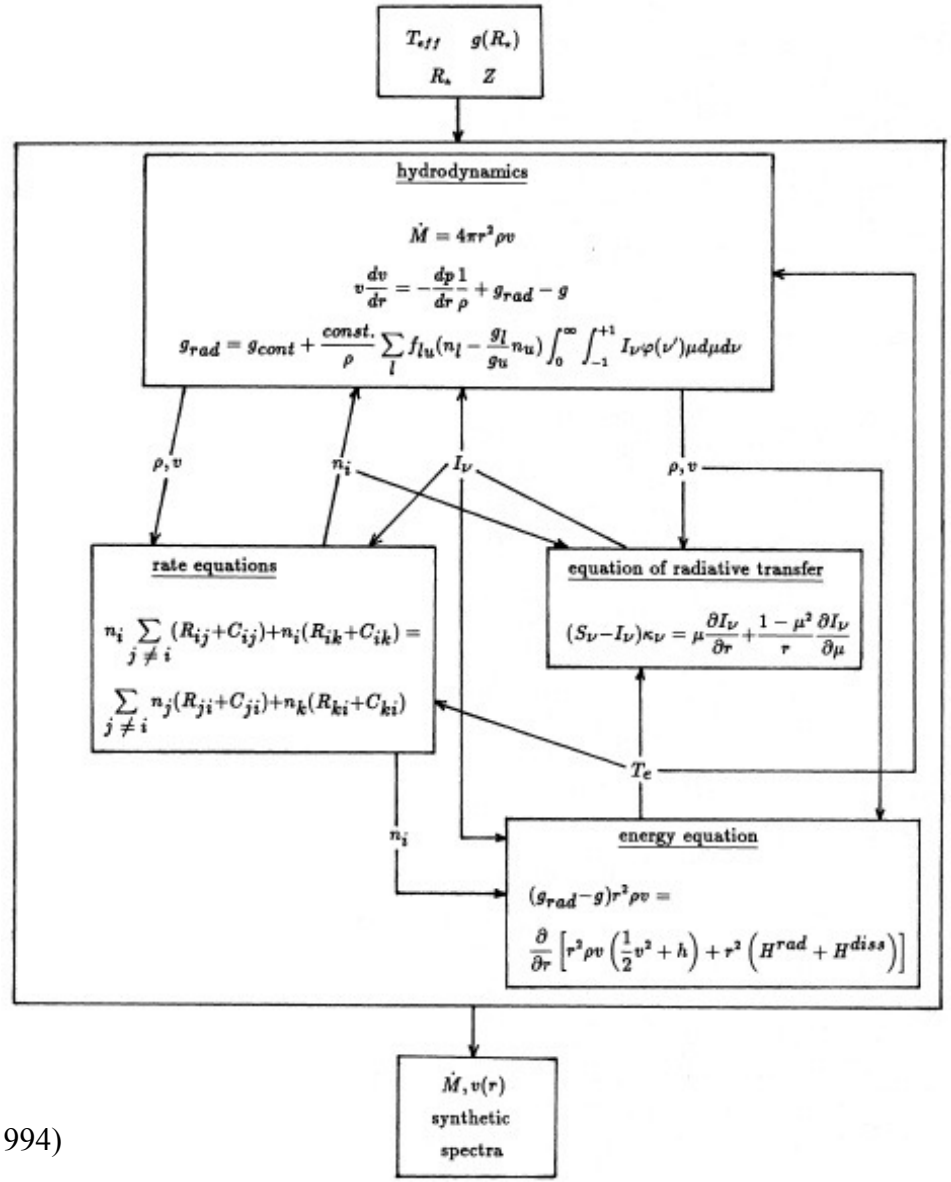

From Pauldrach et al. (1994)

Atmospherical Models

	Detail/Surf. (Butler)	TLUSTY (Hubeny)	Fastwind (Puls)	WM-basic (Pauldrach)	CMFGEN (Hillier)	PoWR (Hamann)	Phoenix (Hauschildt)
geometry	color coding of following Table						
blanketing							
radiative transfer							
temperature structure	optimum treatment (at present state of the art)						
photosphere							
diagnostic range							
major application	less than optimum (but usually faster)						
comments							
execution time							

From J. Puls Lectures
https://www.usm.uni-muenchen.de/people/puls/stellar_at/teneriffa_lectures.pdf
Pages 124-125

Atmospherical Models

	Detail/Surf. (Butler)	TLUSTY (Hubeny)	Fastwind (Puls)	WM-basic (Pauldrach)	CMFGEN (Hillier)	PoWR (Hamann)	Phoenix (Hauschildt)
geometry	plane-parallel	plane-parallel	spherical	spherical	spherical	spherical	spherical/ plane-parallel
blanketing	LTE	yes	approx.	yes	yes	yes	yes
radiative transfer	observer's frame	observer's frame	CMF/ Sobolev	Sobolev	CMF	CMF	CMF/ obs.frame
temperature structure	radiative equilibrium	radiative equilibrium	e^- therm. balance	e^- therm. balance	radiative equilibrium	radiative equilibrium	radiative equilibrium
photosphere	yes	yes	yes	approx.	from TLUSTY	yes	yes
diagnostic range	no limitation	no limitation	optical/IR	UV	no limitation	no limitation	no limitation
major application	hot stars with negl. winds	hot stars with negl. winds	OB-stars, early A-sgs	hot stars with dense winds, ion. fluxes, SNe	OB(A)-stars, WRs, SNe	WRs	stars below 10kK, SNe
comments	no wind	no wind	expl./backgr. elements	no clumping	start model required		molecules incl. no clumping
execution time	few minutes	hour(s)	few minutes to 0.5 h	1 to 2 h	hours	hours	hours

From J. Puls Lectures
https://www.usm.uni-muenchen.de/people/puls/stellar_at/teneriffa_lectures.pdf
Pages 124-125

Quantitative Spectroscopy

Spectral Analysis

Observed Spectrum ⟷ Synthetic Spectrum

Proposal
↑
Detector
↑
Spectrograph
↑
Telescope

Theory of atmospheres

Physical Concepts:
- Atomic Physics
- Hydro/Thermodynamics
- Radiative Transport

Approximations:
- 1-Dimension
- Steady State
- Spherical Symmetry
- etc…

Simulation

Radiative Transport Codes
- NLTE
- CMF calculations

- FASTWIND
- CMFGEN
- POWR

Input:
- Stellar Parameters
- Wind Parameters
- Abundances

Spectral Analysis

Comparison by
"eye inspection"

Observed Spectrum ⟷ Synthetic Spectrum

Proposal
↑
Detector
↑
Spectrograph
↑
Telescope

Theory of atmospheres

Physical Concepts:
- Atomic Physics
- Hydro/Thermodynamics
- Radiative Transport

Approximations:
- 1-Dimension
- Steady State
- Spherical Symmetry
- etc…

Simulation

Radiative Transport Codes
- NLTE
- CMF calculations

- FASTWIND
- CMFGEN
- POWR

Input:
- Stellar Parameters
- Wind Parameters
- Abundances

B Supergiant winds

"Eye inspection"

Monthly Notices of the ROYAL ASTRONOMICAL SOCIETY

MNRAS **527,** 93–111 (2024)
Advance Access publication 2023 October 31

https://doi.org/10.1093/mnras/stad3030

The wind of rotating B supergiants – II. The δ-slow hydrodynamic regime

R. O. J. Venero [1,2★] M. Curé,[3★] J. Puls,[4] L. S. Cidale,[1,2★†] M. Haucke,[5] I. Araya [6] A. Gormaz-Matamala[7,8,9] and C. Arcos [3]

[1]*Departamento de Espectroscopía, Facultad de Ciencias Astronómicas y Geofísicas, Universidad Nacional de La Plata, Paseo del Bosque S/N, BF1900FWA La Plata, Buenos Aires, Argentina*
[2]*Instituto de Astrofísica de La Plata, CCT La Plata, CONICET-UNLP, Paseo del Bosque S/N, BF1900FWA La Plata, Buenos Aires, Argentina*
[3]*Instituto de Física y Astronomía, Facultad de Ciencias, Universidad de Valparaíso, Av. Gran Bretaña 1111, Casilla 5030, Valparaíso, Chile*
[4]*LMU München, University Observatory, Scheinerstr. 1, 81679 München, Germany*
[5]*Facultad de Ingeniería, Universidad Nacional de La Plata, Av. 1 No. 750, B1900TAG La Plata, Buenos Aires, Argentina*
[6]*Centro Multidisciplinario de Física, Vicerrectoría de Investigación, Universidad Mayor, 8580745 Santiago, Chile*
[7]*Nicolaus Copernicus Astronomical Center, Polish Academy of Sciences, ul. Bartycka 18, 00-716 Warsaw, Poland*
[8]*Departamento de Ciencias, Facultad de Artes Liberales, Universidad Adolfo Ibáñez, Av. Padre Hurtado 750, Viña del Mar, Chile*
[9]*Instituto de Astrofísica, Facultad de Física, Pontificia Universidad Católica de Chile, 782-0436 Santiago, Chile*

ISOSCELES: B Supergiant winds

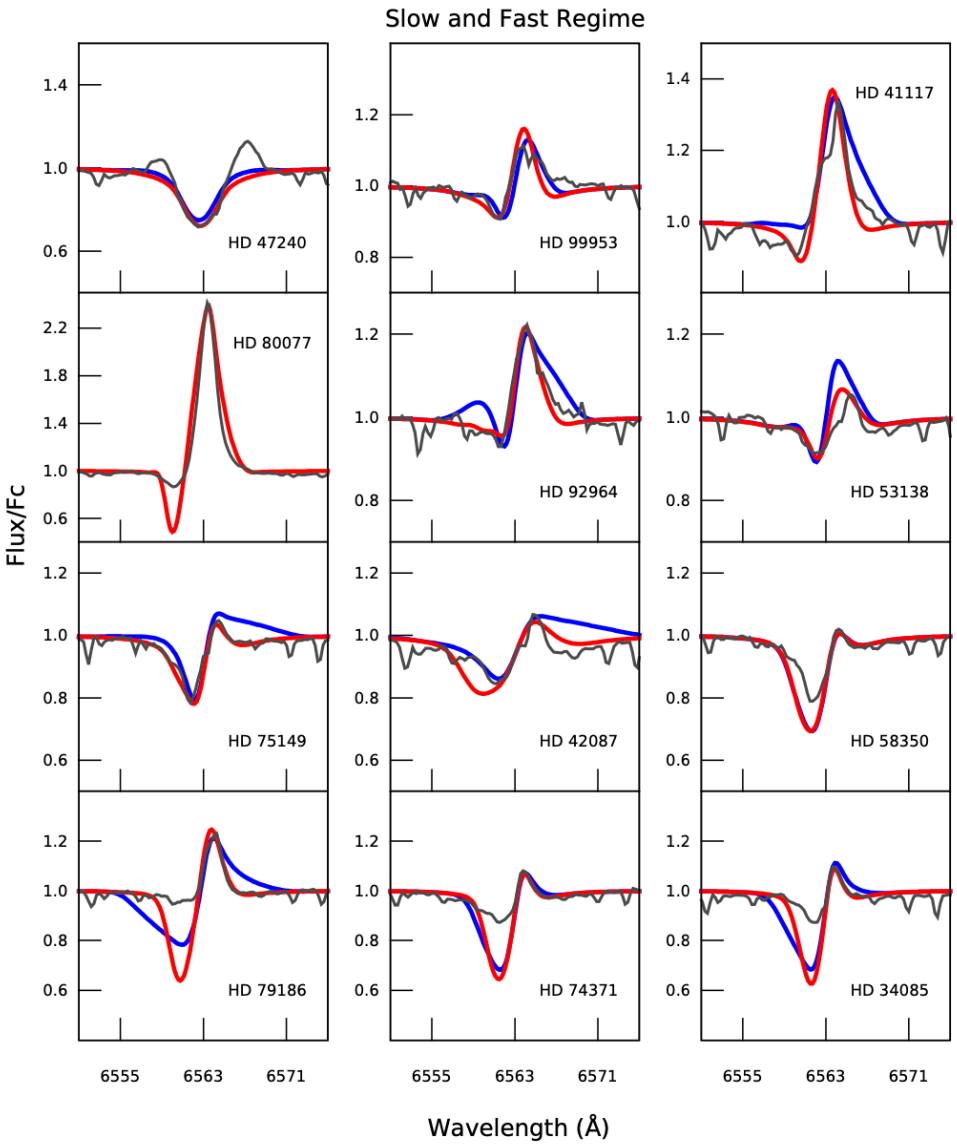

Figure 10. Hα line profile fits for selected B supergiants using δ-*slow* (red) and *fast* (blue) hydrodynamical models. The corresponding stellar and wind parameters are given in Tables 2 and 3, respectively. In the case of HD 80077, we could not find a *fast* solution. The line profiles calculated for the *fast* and *slow* regimes for the star HD 58350 exactly overlap.

Synthetic spectral database

POEMS

GrId of Stellar atmOSphere and hydrodynamiC modELs of massivE Stars

Araya et al. 2023 Winds of Stars and Exoplanets.
Proceedings of the International Astronomical Union, Volume 370, pp. 180-184

ISOSCELES: HYDWIND

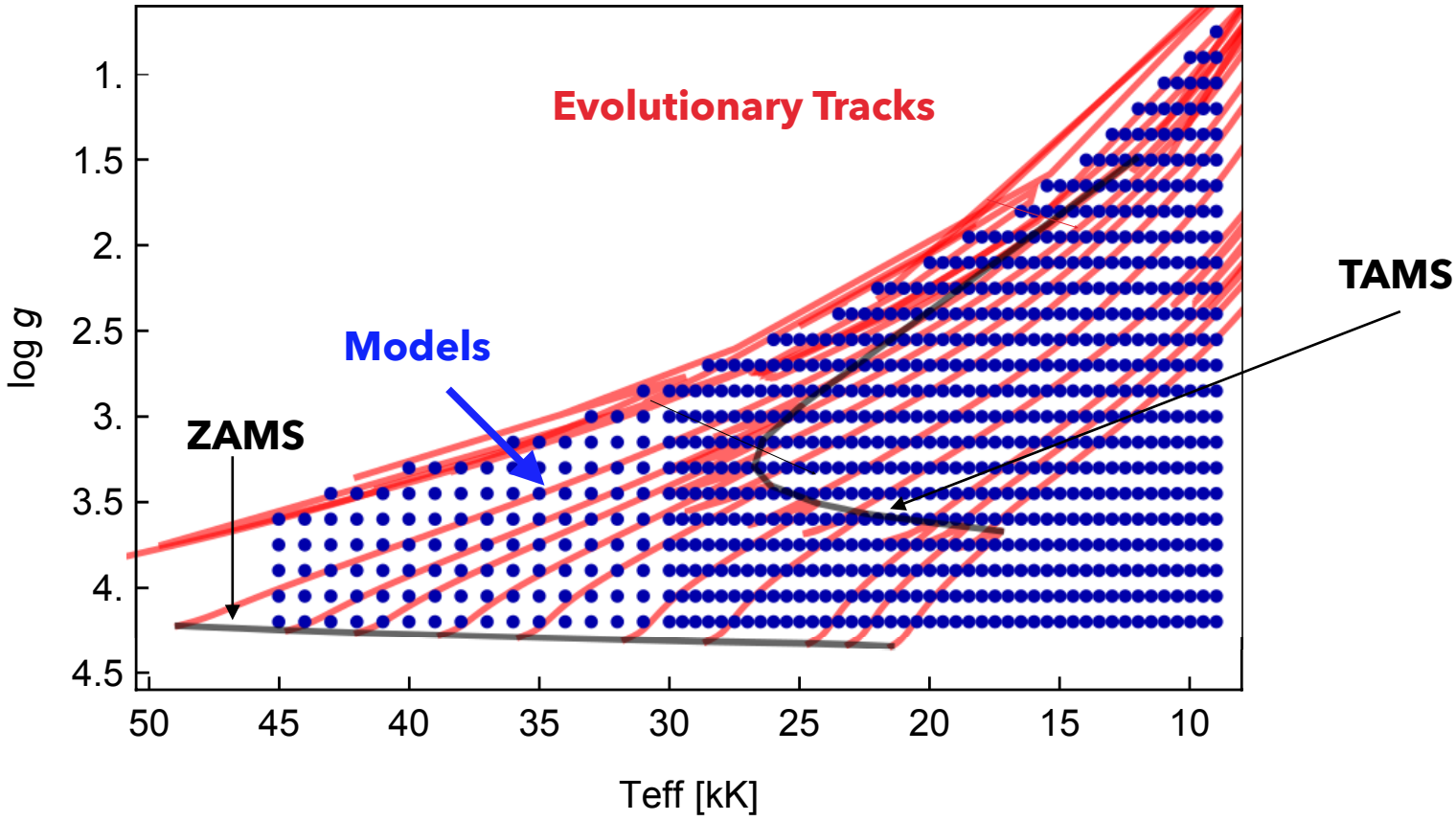

4 056 755 converged models

ISOSCELES: FASTWIND

Fastwind grid (without rotation)

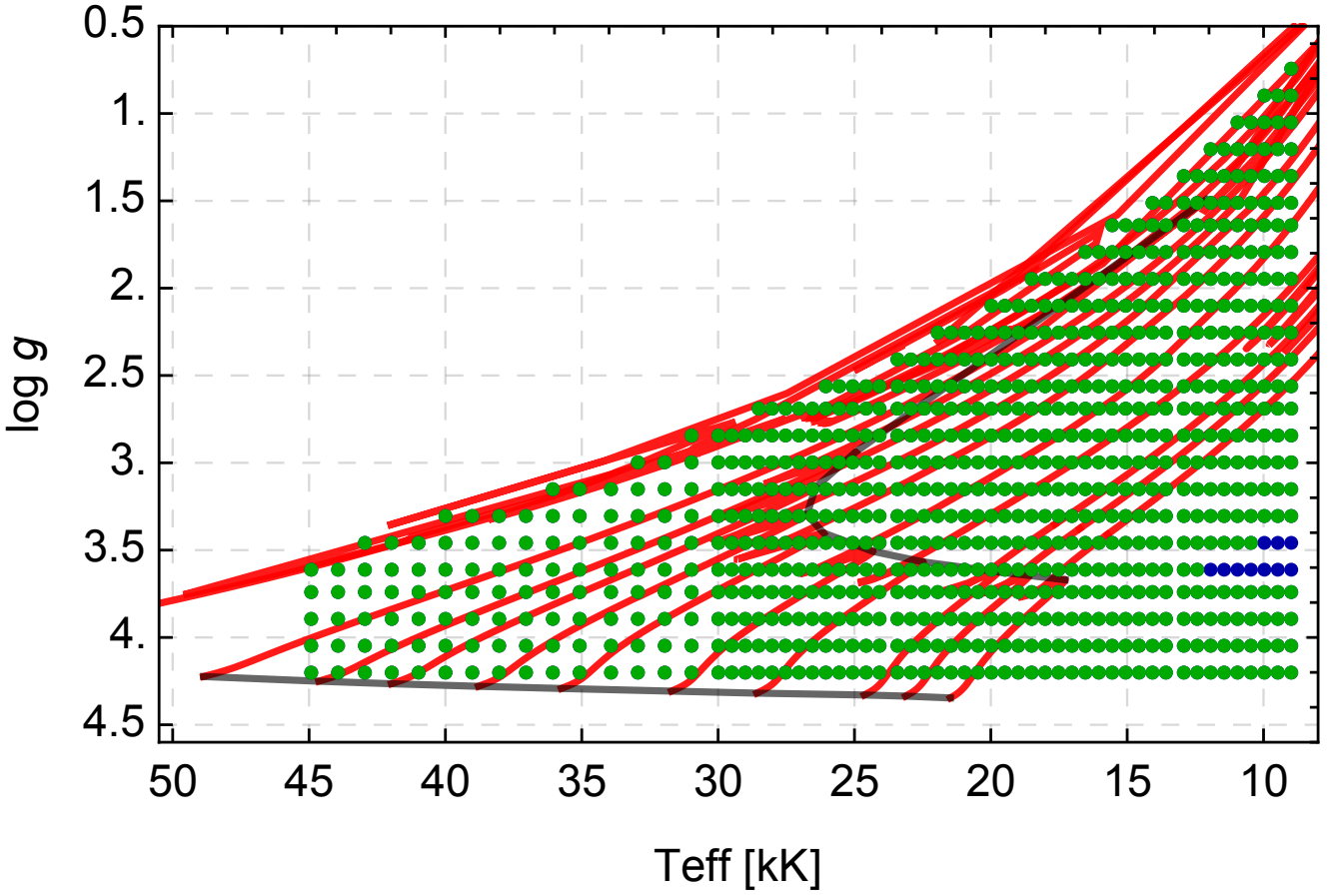

Total = 573 423 converged models

ISOSCELES: Grid parameters

Temperature

9 kK - 30 kK (steps of 500 k)
31 kK - 45 kK (steps of 1000 k)

log g

4.2 - 0.75 (steps of 0.15)

Line force parameters

α	0.45	0.47	0.51	0.53	0.55	0.57	0.61	0.65				
k	0.05	0.1	0.15	0.2	0.25	0.3	0.35	0.4	0.45	0.5	0.55	0.6
δ	0.	0.04	0.1	0.14	0.2	0.24	0.3	0.31	0.32	0.33	0.34	0.35

Si abundance log ϵ_{Si}

7.21, 7.36, 7.51 (solar), 7.66, and 7.81 dex.

Micro-turbulent velocity

1, 5 , 10, 15, 20, 25 km/s

"New" Quantitative Spectroscopy

Spectral Analysis via Machine Learning

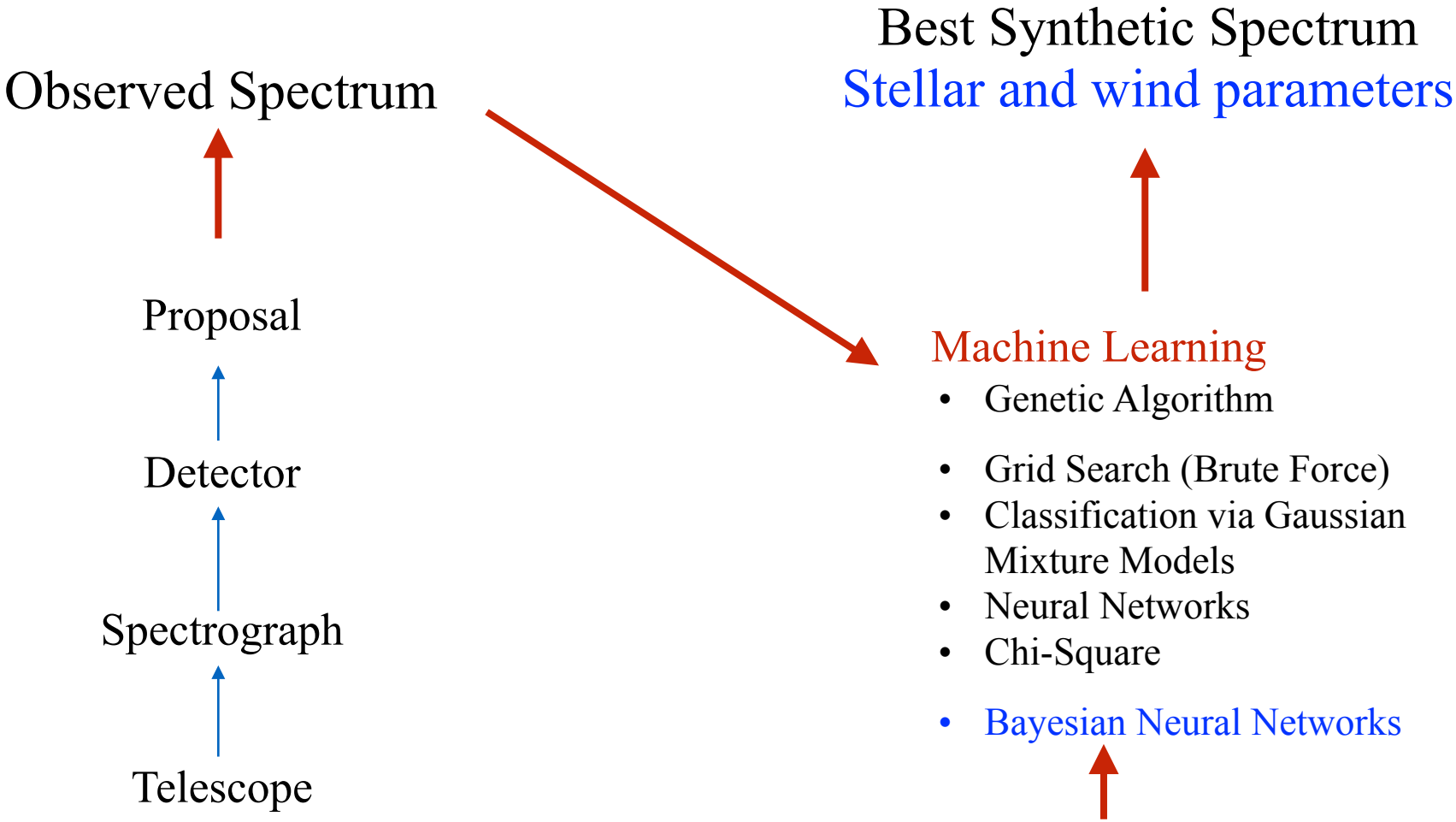

ISOSCELES: Grid Search

Natalia Machuca PhD thesis UV

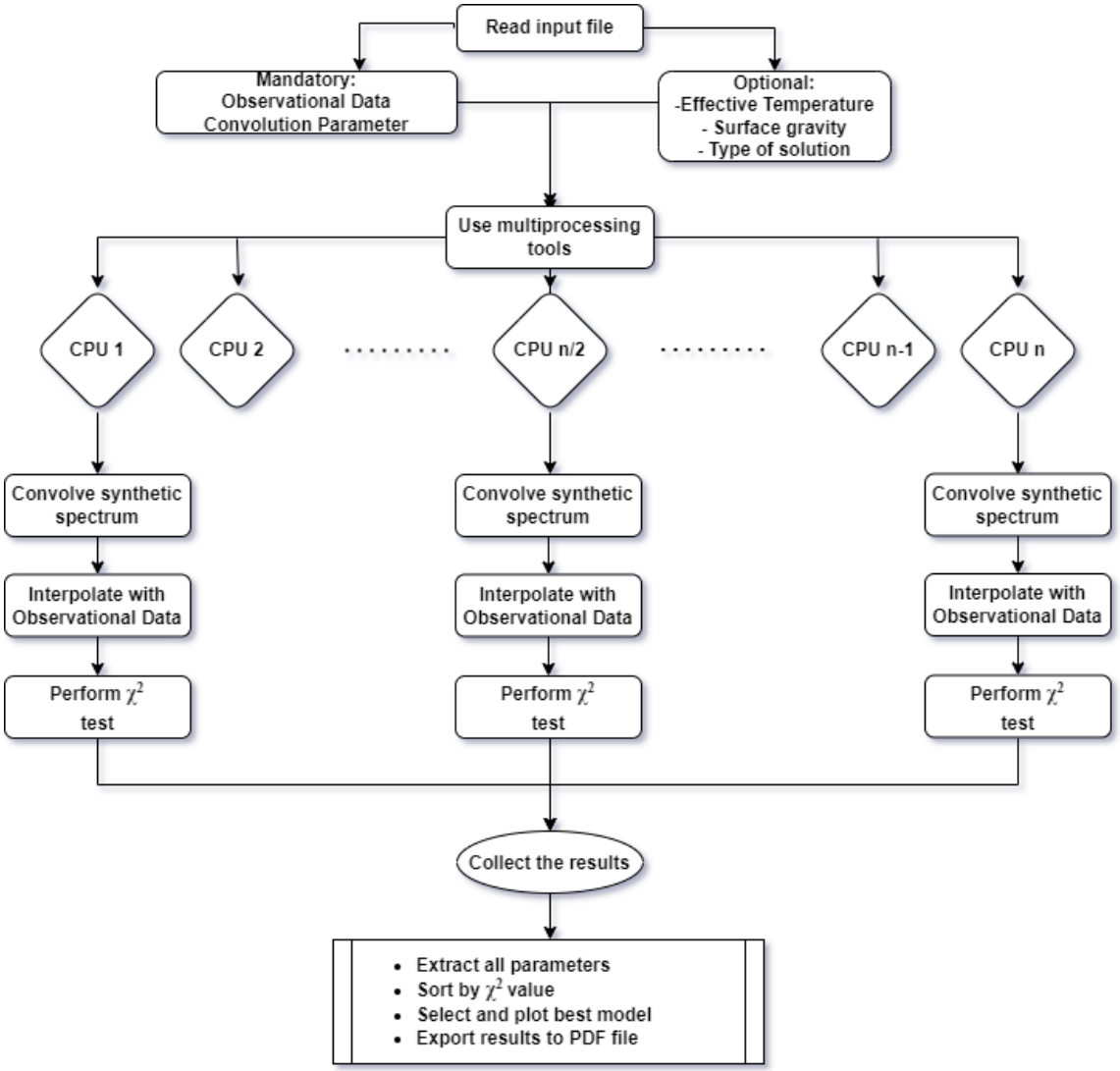

ISOSCELES: First Results

HD 146333 (O8.5 V). Fast solution

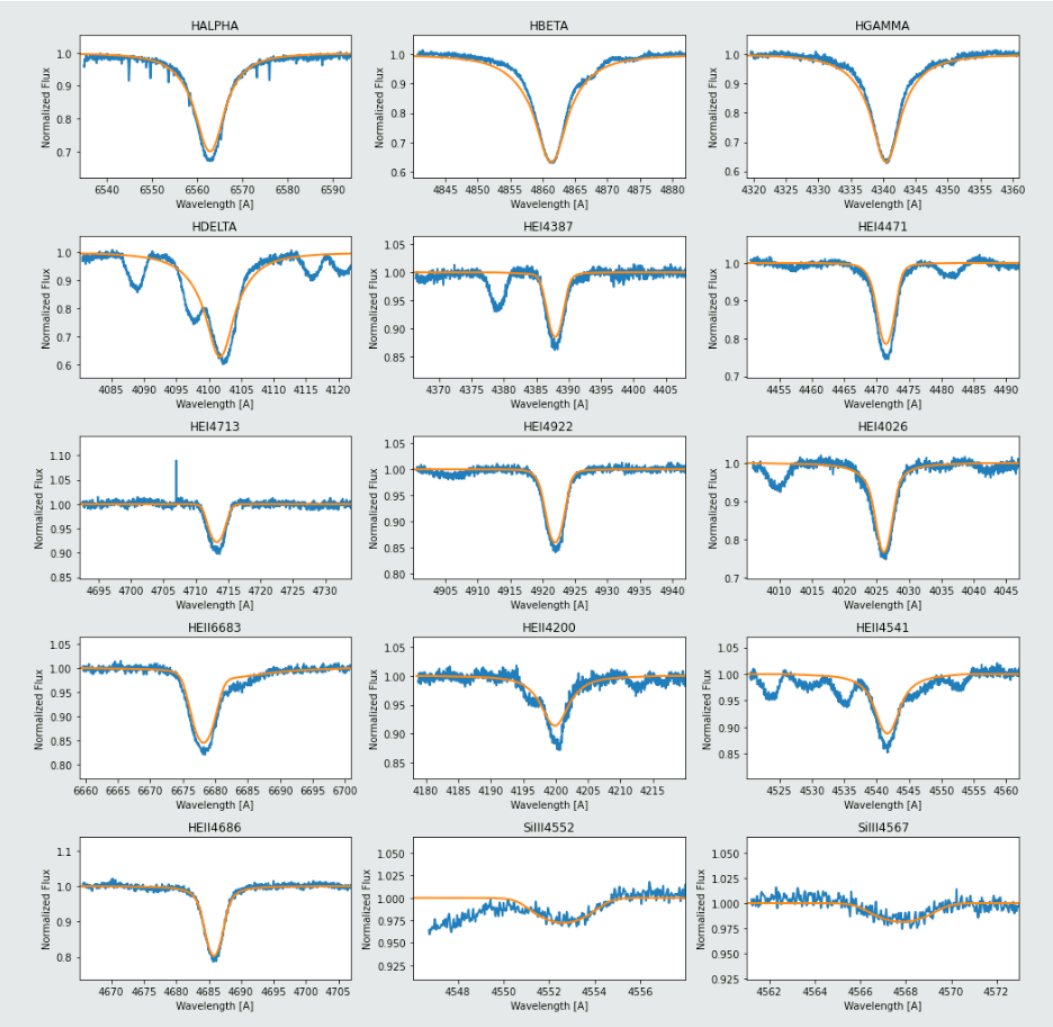

$T_{eff} = 36000$ K
$\log g = 4.05$

$\alpha = 0.51$
$k = 0.30$
$\delta = 0.10$

$\dot{M} = 3.08 \times 10^{-8} M_{\odot}/yr$
$v_{\infty} = 597.41$ km/s

Observations from Haucke et al. 2018

ISOSCELES: First Results

HD 99953

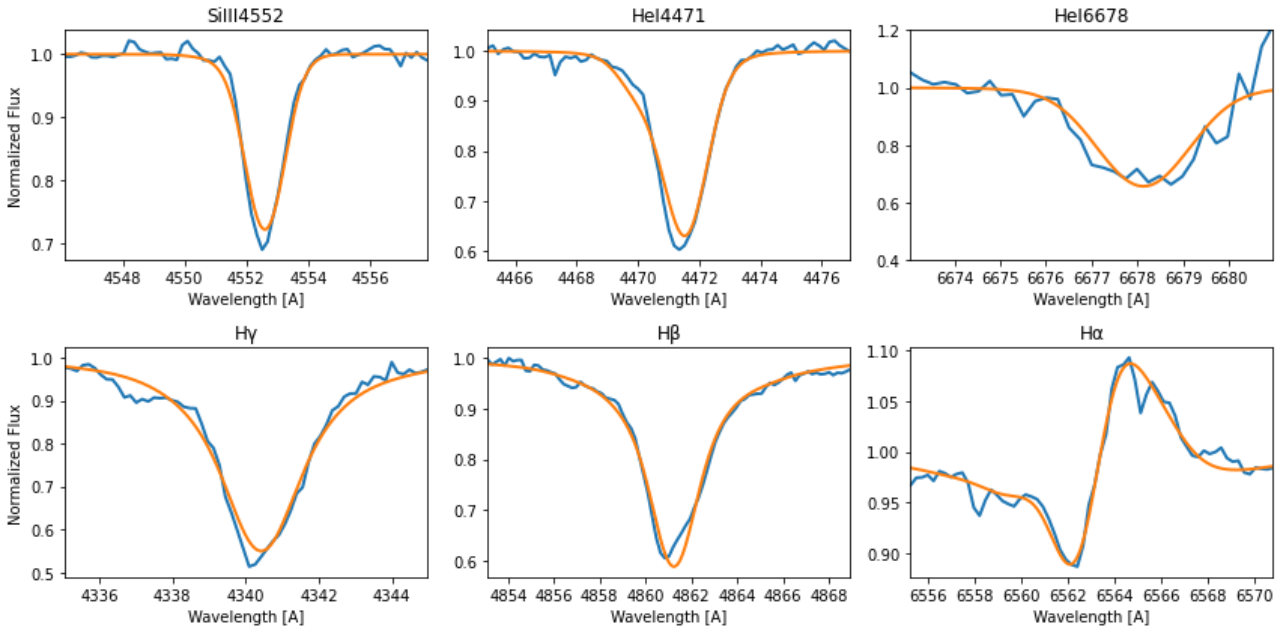

	Haucke et al. 2018	This work
T_{eff} [K]	19000	18500
log *g*	2.30	2.40
α	–	0.53
k	–	0.15
δ	–	**0.34**
β	2.0	–
$\dot{M}$ [10^{-6} $M_\odot$ / yr]	0.13	0.24
v_∞ [km/s]	500	254

Observations from Haucke et al. 2018

WML relationship

Since the stellar winds of massive stars are driven by radiation, it is reasonable to expect that the mechanical momentum of the flowing material is related to the momentum of the radiation field.

Wind Momentum Definition

$$D_{\rm mom} = \dot{M}\, v_\infty \sqrt{R_*/R_\odot}$$

Wind momentum Luminosity Relationship

$$D_{\rm mom} \propto \left(\frac{L}{L_\odot}\right)^x$$

WML relationship

$$\dot{M}\, v_\infty \propto \frac{1}{\sqrt{R_*}} L^x$$

Kudritzki et al. 1999

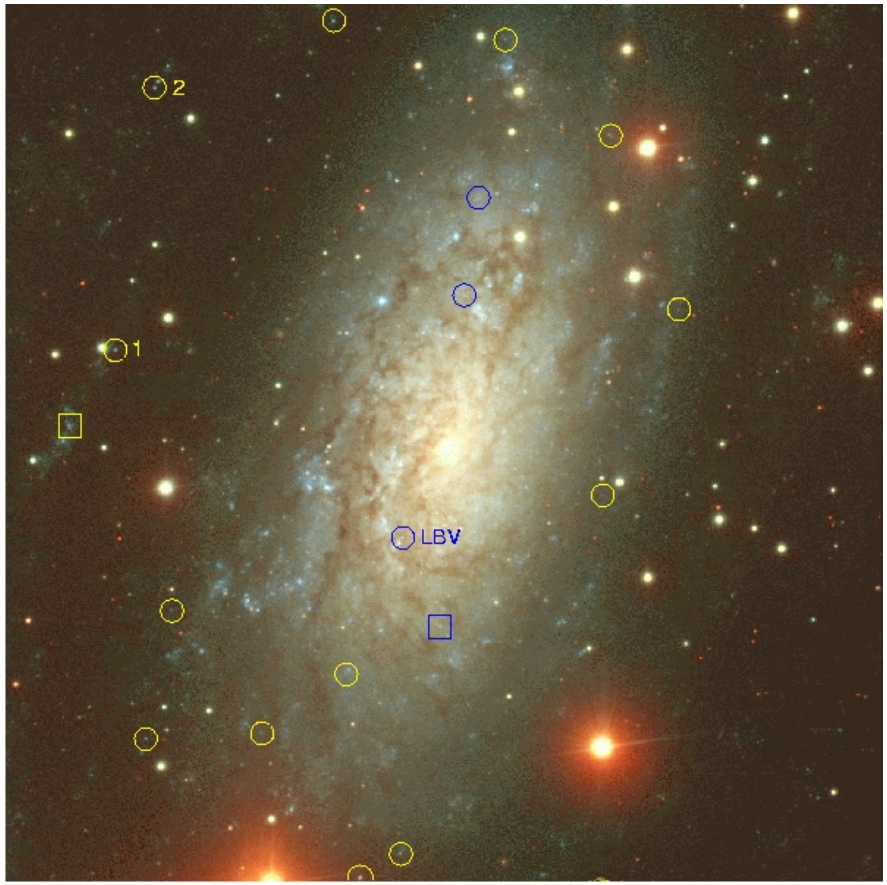

NGC3621

WML relationship

Kudritzki et al. 1999

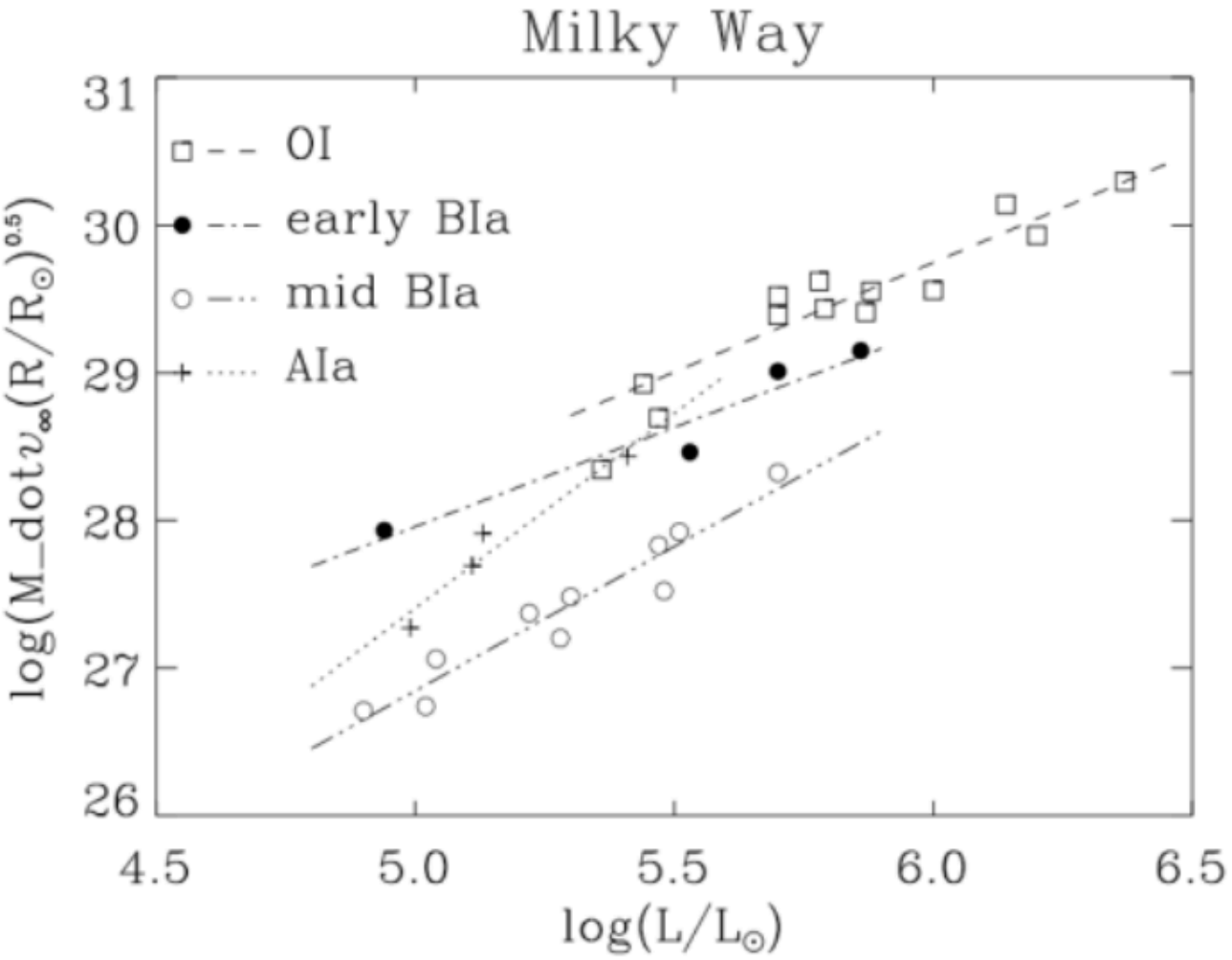

ISOSCELES:WML relationship

Natalia Machuca PhD tesis UV: work in progress, 100 OB stars analised

ISOSCELES:WML relationship

Natalia Machuca PhD tesis UV: work in progress, 100 OB stars analised

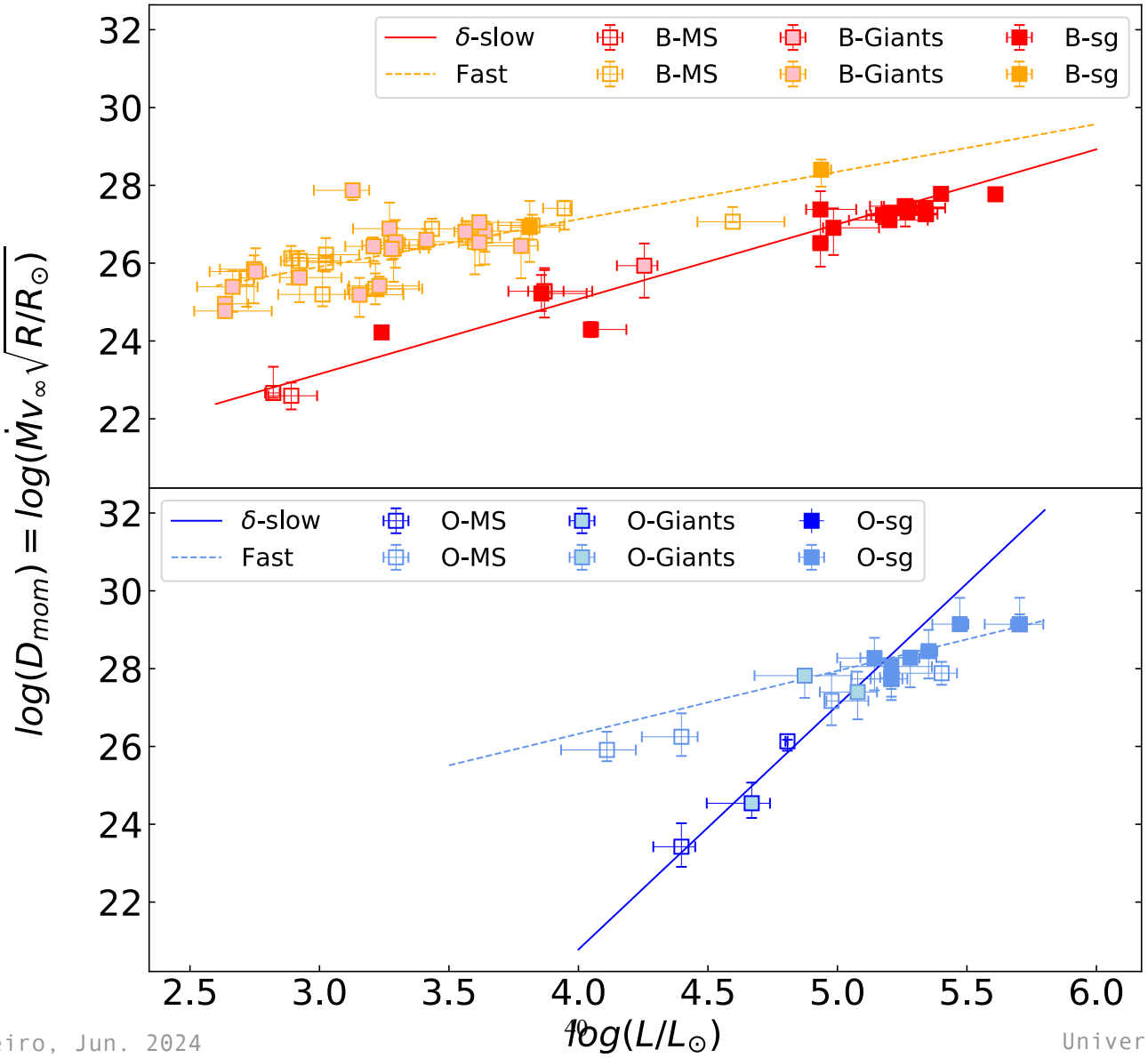

Michel Curé
Universidad de Valparaíso

ISOSCELES:WML relationship

Natalia Machuca PhD tesis UV: work in progress, 100 OB stars analised

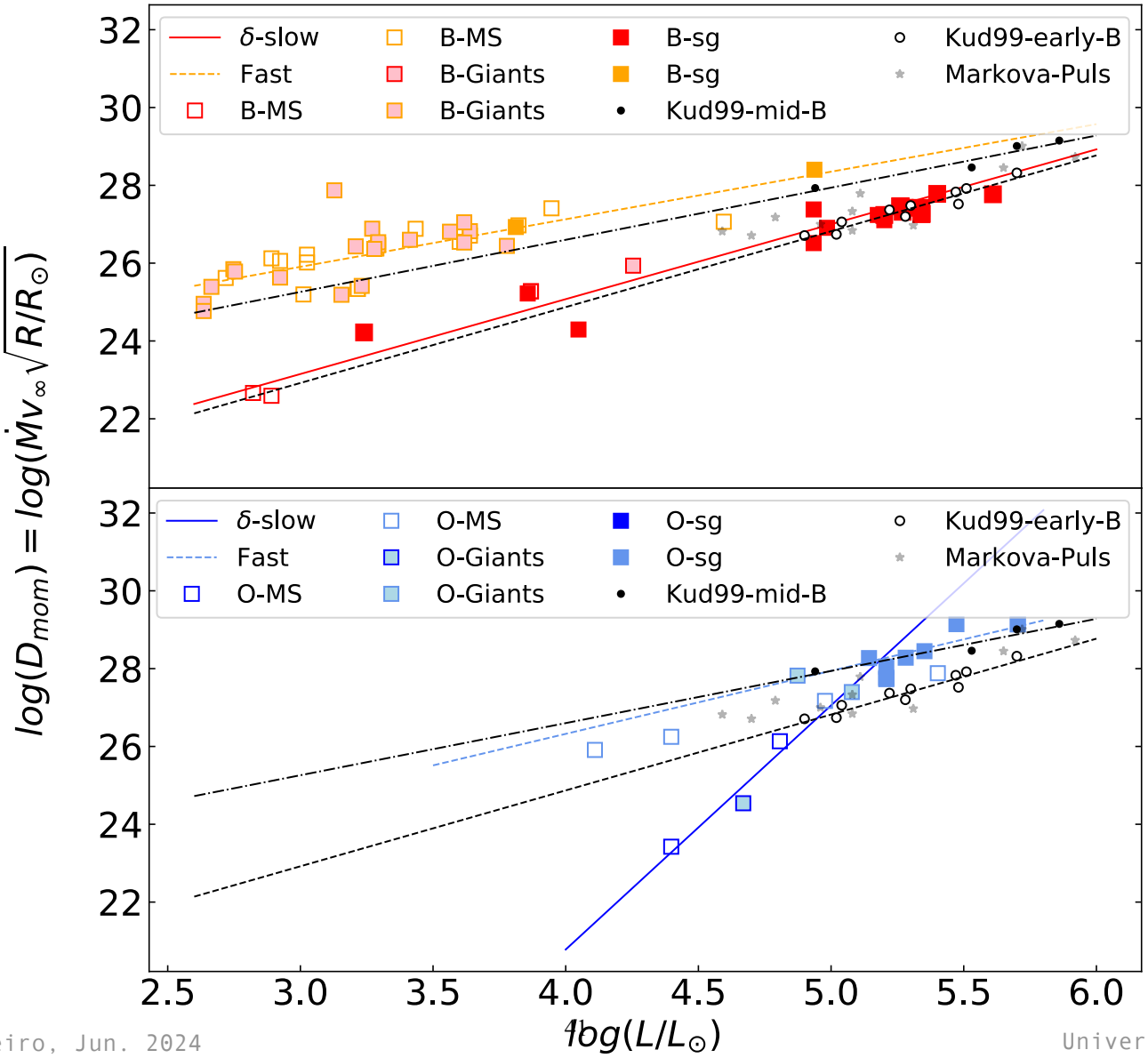

Michel Curé
Universidad de Valparaíso

ISOSCELES Grid
&
Machine Learning

ISOSCELES: Machine Learning

Gaussian Mixture Model Classification,
Neural Networks and "Brut" force:
ISOSCELES' δ-Slow Wind Solutions (~330000 models)
Hα spectral line

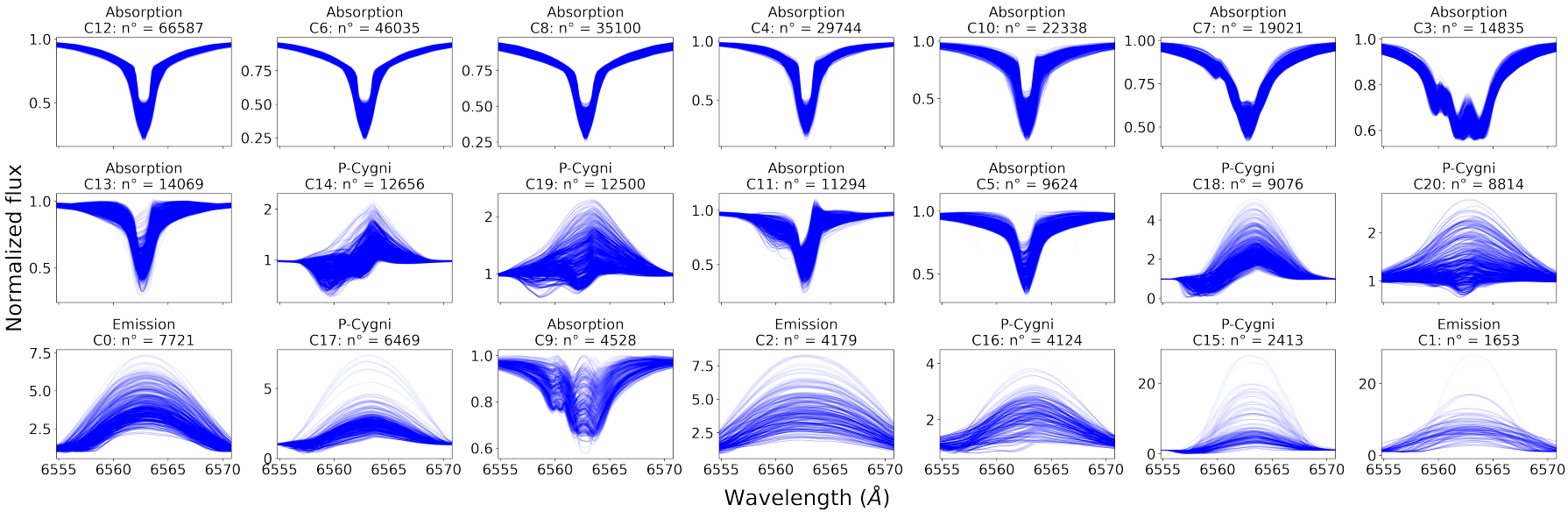

Felipe Ortiz Master's thesis UV

ISOSCELES: Machine Learning

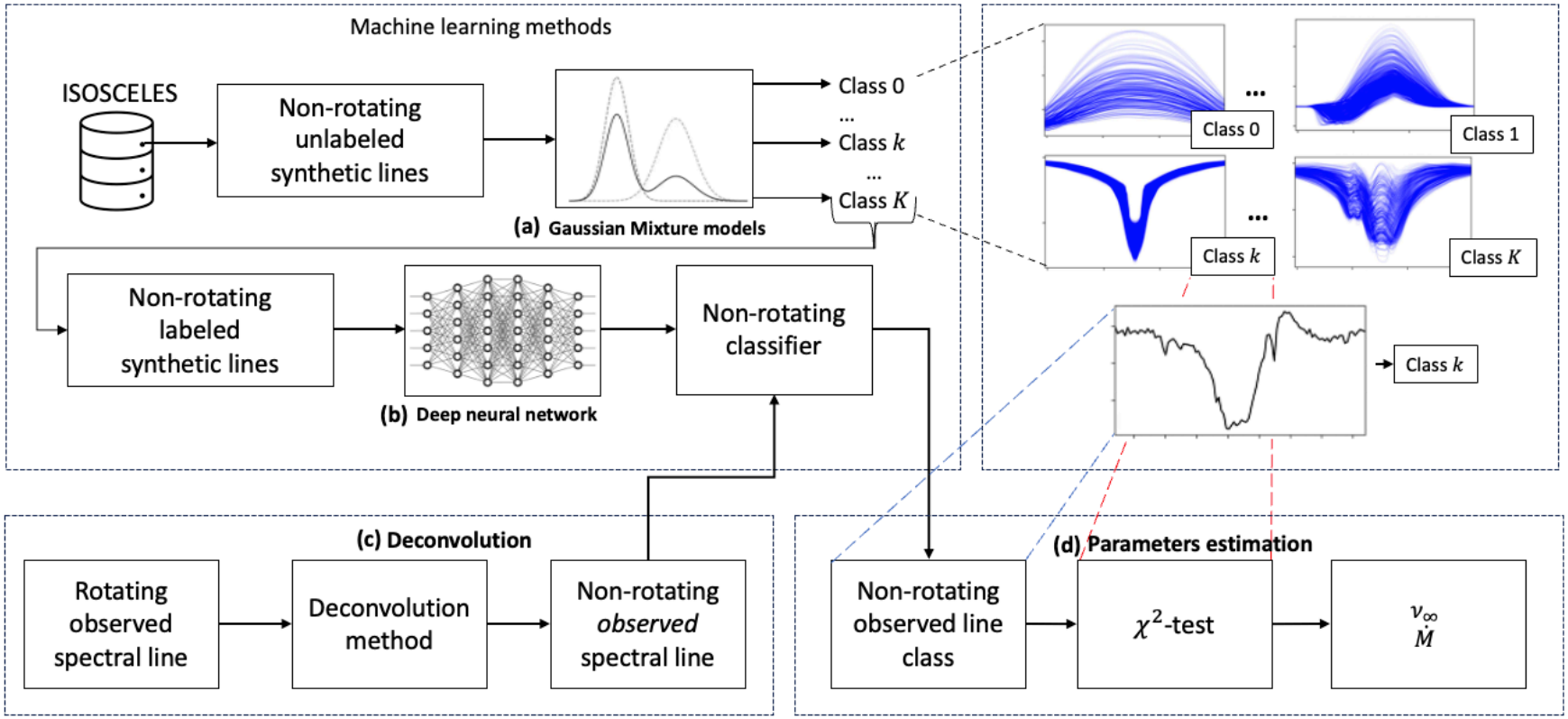

ISOSCELES: B Supergiant winds

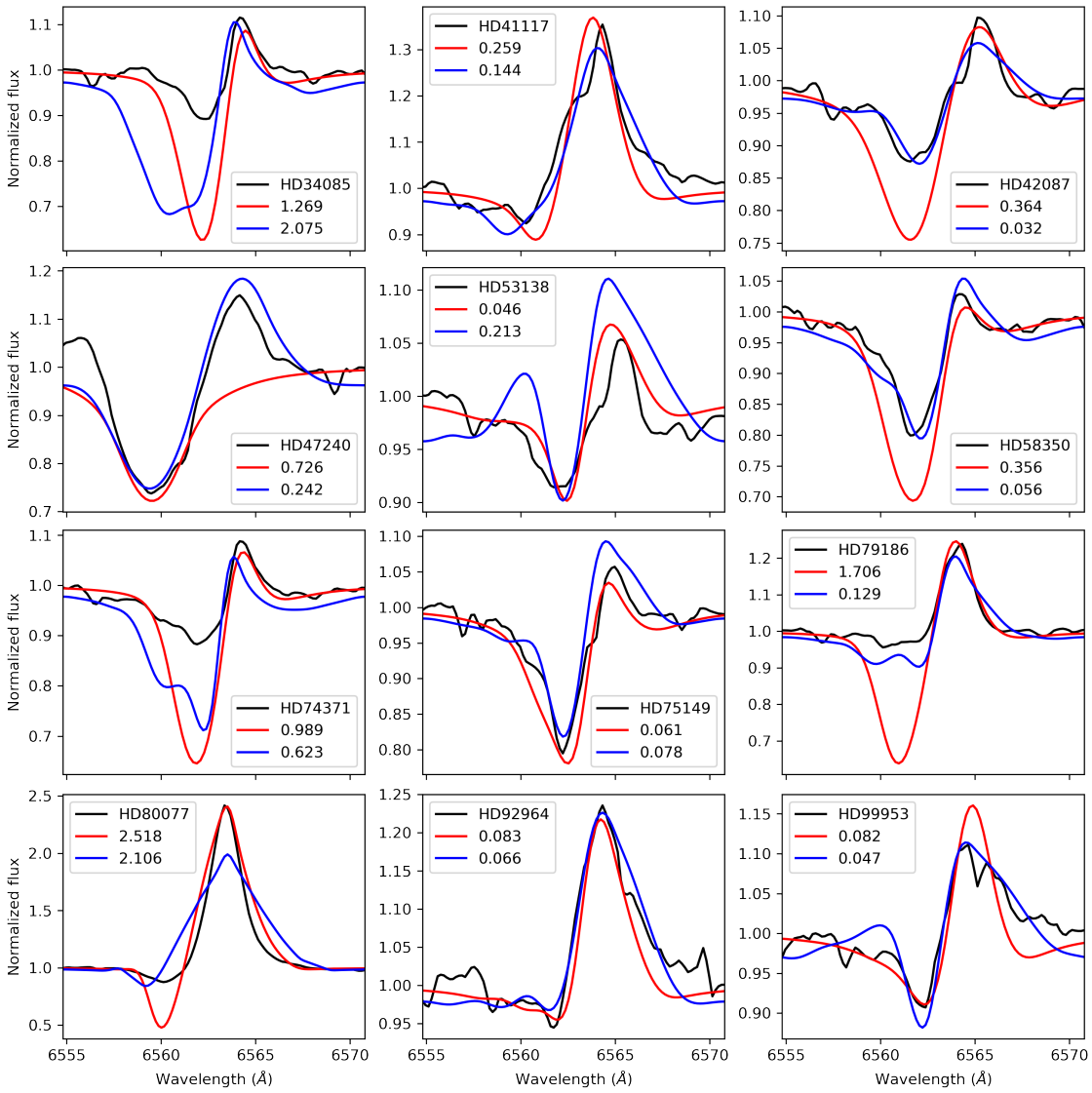

Ortiz et al. 2024, Astronomy and Computing

Submmitted

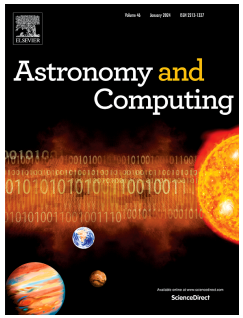

ISOSCELES: B Supergiant winds

Improvements in 9 of the 12 B-supergiants

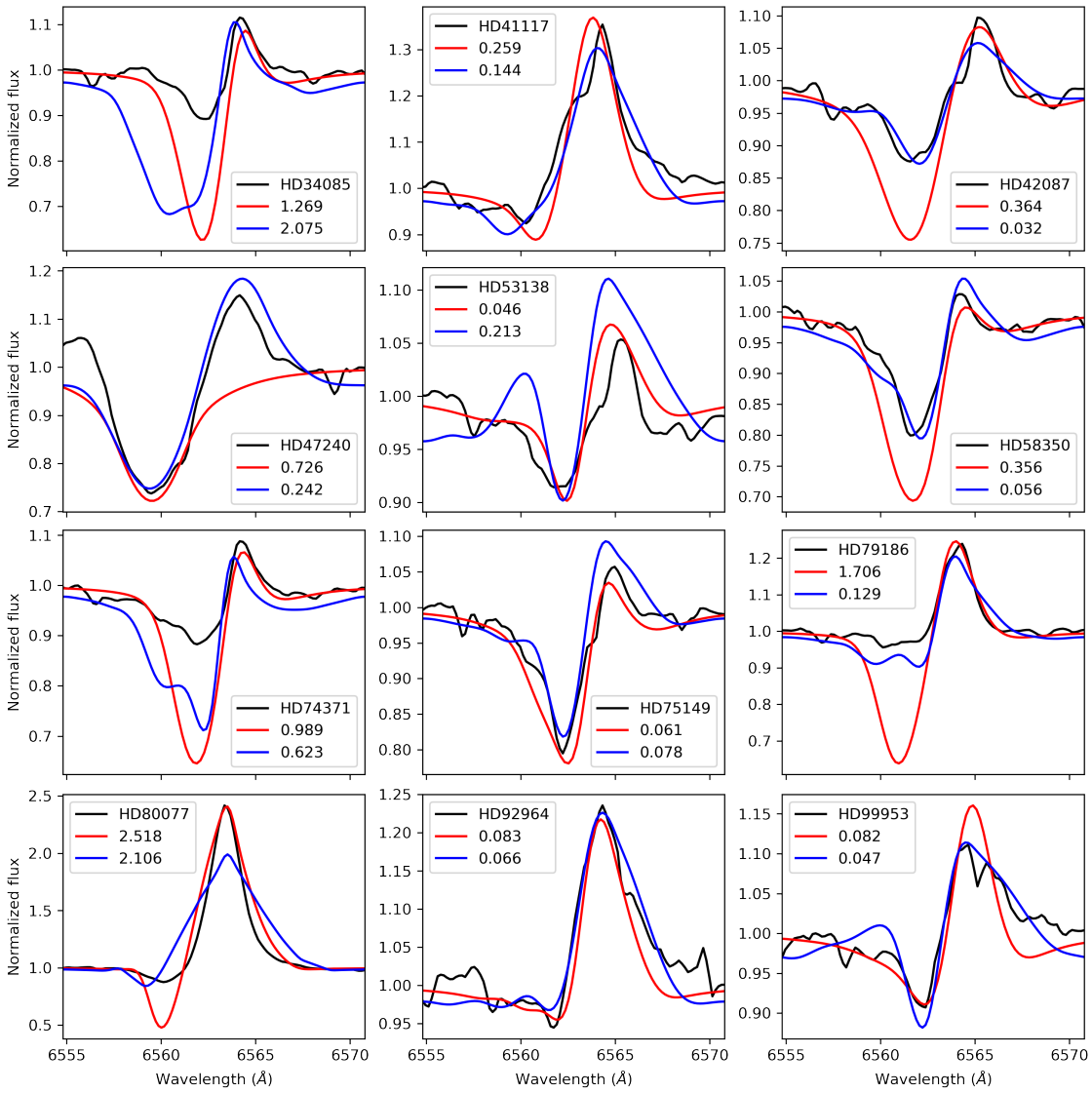

Ortiz et al. 2024, Astronomy and Computing

Submmitted

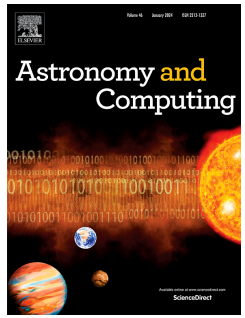

Bayesian Neural Networks

Monte Carlo Dropout

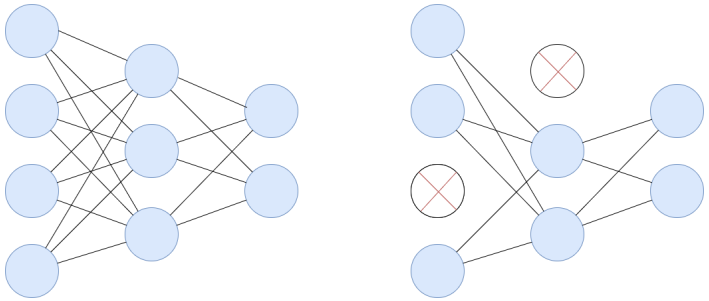

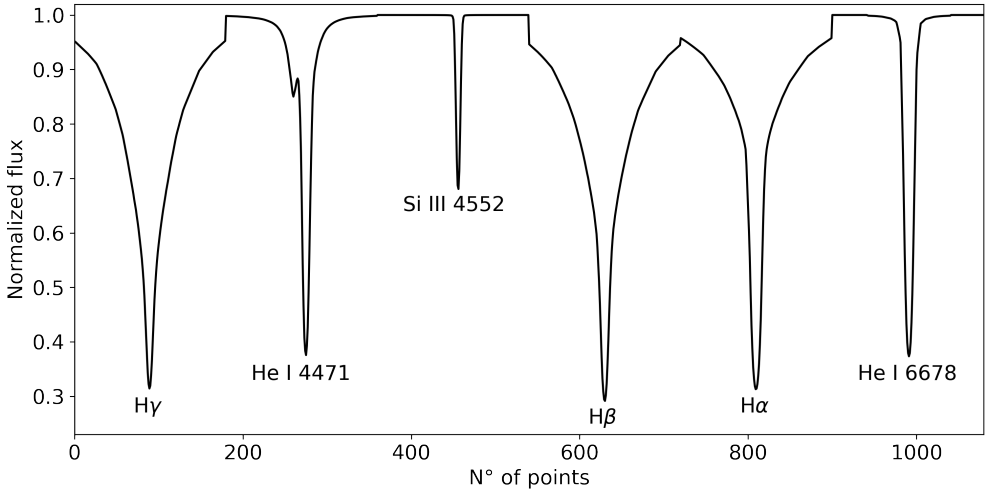

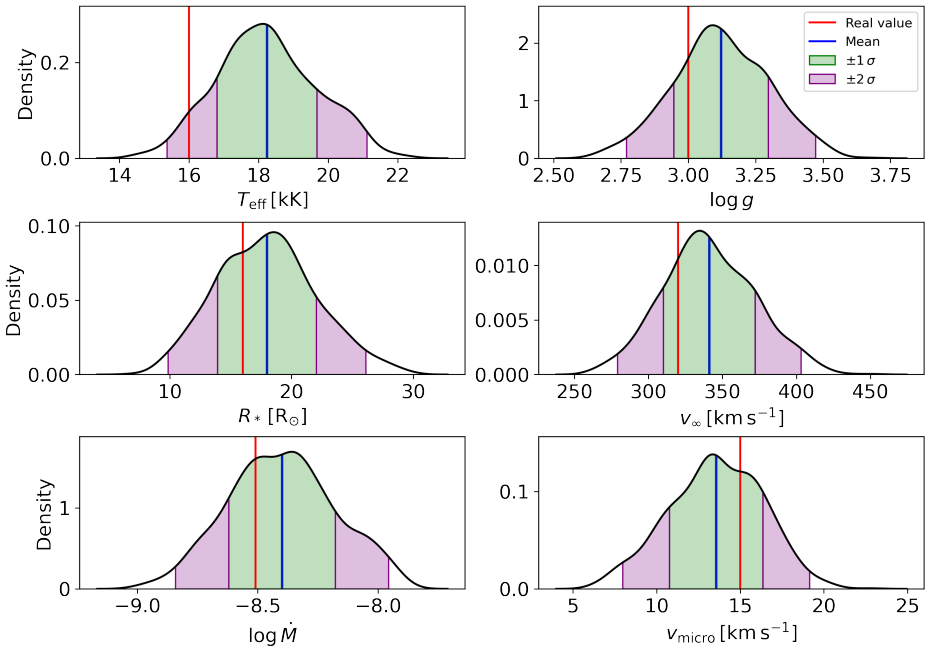

Felipe Ortiz PhD thesis UV

ISOSCELES

- ISOSCELES is the first grid of synthetic data for massive stars that involves both, the m-CAK hydrodynamics and the NLTE radiative transport.
- Calculate new grids including UV range for different metallicities
- The results obtained from ISOSCELES should have a better justification than the currently and widely calculated models with a β-law in quantitative spectroscopic analyses, specially for high values of β
- We are analysing the x^2 distributions and then use them to compute the uncertainties for each derived parameter
- More fast and efficient "searching" algorithms (Machine Learning)
- Bayesian Neural Networks, etc.

The Lambert-W procedure

The Astrophysical Journal, 920:64 (30pp), 2021 October 10 https://doi.org/10.3847/1538-4357/ac12c9

New Hydrodynamic Solutions for Line-driven Winds of Hot Massive Stars Using the Lambert *W*-function

A. C. Gormaz-Matamala[1,2,3], M. Curé[1,2], D. J. Hillier[4], F. Najarro[5], B. Kubátová[6], and J. Kubát[6]
[1] Instituto de Física y Astronomía, Universidad de Valparaíso, Av. Gran Bretaña 1111, Casilla 5030, Valparaíso, Chile; alex.gormaz@uv.cl
[2] Centro de Astrofísica, Universidad de Valparaíso, Av. Gran Bretaña 1111, Casilla 5030, Valparaío, Chile
[3] Departamento de Ciencias, Facultad de Artes Liberales, Universidad Adolfo Ibáñez, Av. Padre Hurtado 750, Viña del Mar, Chile
[4] Department of Physics and Astronomy & Pittsburgh Particle Physics, Astrophysics, and Cosmology Center (PITT PACC), University of Pittsburgh, Pittsburgh, PA 15260, USA
[5] Centro de Astrobiología (CSIC/INTA), ctra. de Ajalvir km. 4, E-28850 Torrejón de Ardoz, Madrid, Spain
[6] Astronomickýústav, Akademie věd České republiky, 251 65 Ondřejov, Czech Republic
Received 2021 February 16; revised 2021 June 25; accepted 2021 June 28; published 2021 October 13

Abstract

Hot massive stars present strong stellar winds that are driven by absorption, scattering, and reemission of photons by the ions of the atmosphere (line-driven winds). A better comprehension of this phenomenon, and a more accurate calculation of hydrodynamics and radiative acceleration, is Required to reduce the number of free parameters in spectral fitting and to determine accurate wind parameters such as mass-loss rates and velocity profiles. We use the non-LTE model-atmosphere code CMFGEN to numerically solve the radiative transfer equation in the stellar atmosphere and to calculate the radiative acceleration $g_{\rm rad}(r)$. Under the assumption that the radiative acceleration depends only on the radial coordinate, we solve analytically the equation of motion by means of the Lambert *W*-function. An iterative procedure between the solution of the radiative transfer and the equation of motion is executed in order to obtain a final self-consistent velocity field that is no longer based on any β-law. We

Radiation Driven Wind Hydrodynamics

Mass Conservation

$$\dot{M} = 4\,\pi\, r^2\, \rho\, v$$

Momentum Conservation

$$v\,\frac{dv}{dr} = -\frac{1}{\rho}\,\frac{dP}{dr} - \frac{G\,M\,(1-\Gamma)}{r^2} + g^{line}\left(\rho, \frac{dv}{dr}, n_e\right)$$

Michel Curé
Universidad de Valparaíso

Radiation Driven Wind Hydrodynamics

POEMS

Mass Conservation

$$\dot{M} = 4\,\pi\, r^2\, \rho\, v$$

Momentum Conservation

$$v\,\frac{dv}{dr} = -\frac{1}{\rho}\,\frac{dP}{dr} - \frac{G\,M\,(1-\Gamma)}{r^2} + g^{line}\left(\rho, \frac{dv}{dr}, n_e\right)$$

DEPARTAMENTO FISICA Y Astronomia

Radiation Driven Wind Hydrodynamics

Mass Conservation

$$\dot{M} = 4\pi r^2 \rho v$$

Momentum Conservation

$$v\frac{dv}{dr} = -\frac{1}{\rho}\frac{dP}{dr} - \frac{GM(1-\Gamma)}{r^2} + g^{line}\left(\rho, \frac{dv}{dr}, n_e\right)$$

$g^{line}(r)$

The Lambert-W procedure

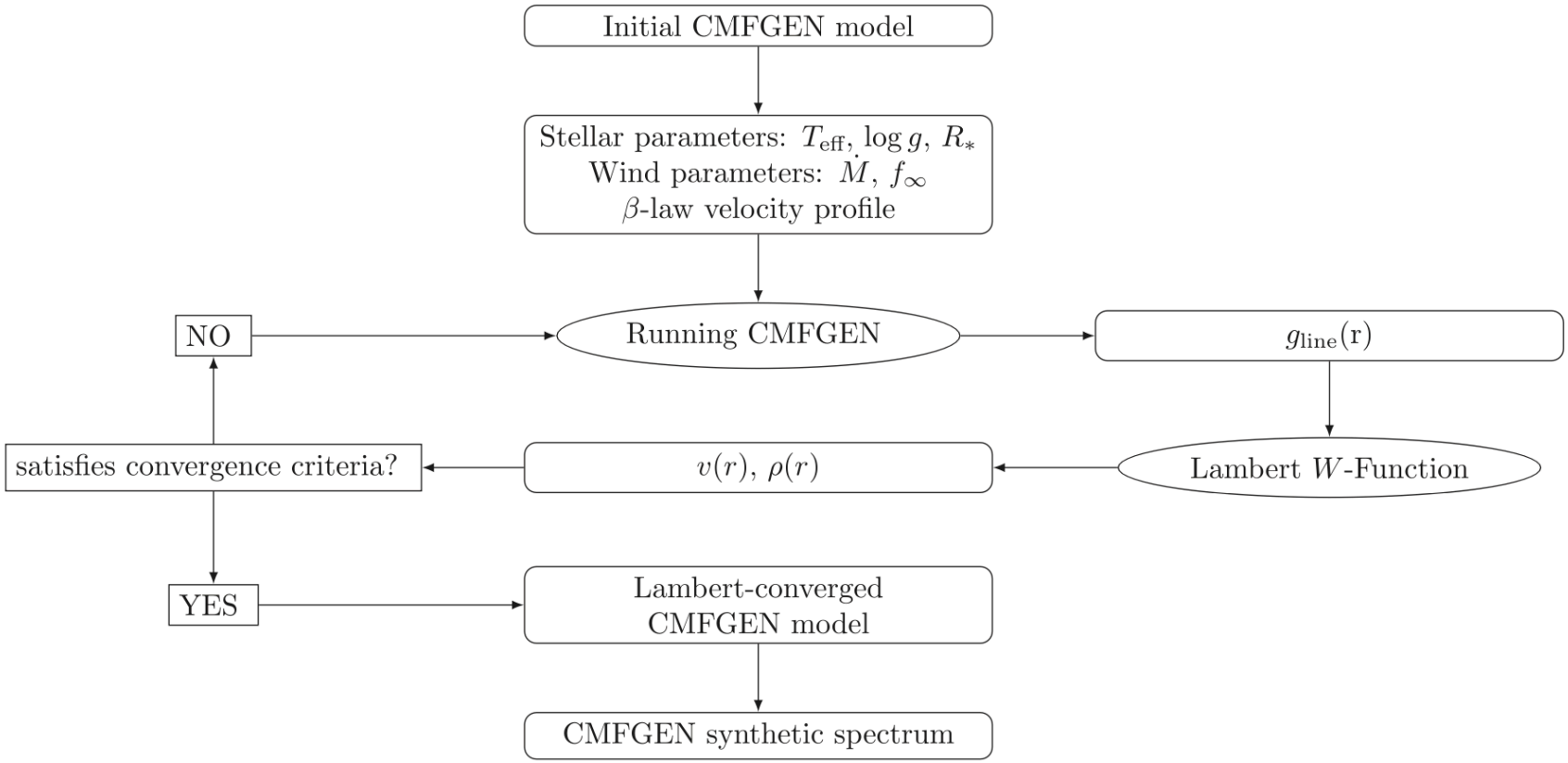

The Lambert-W procedure

ζ Puppis parameters

Table 2

Summary of Self-consistent Solutions Performed by Sander et al. (2017), Gormaz-Matamala et al. (2019), and This Present Study (Table 1)

	Sander et al. (2017)	Gormaz-Matamala et al. (2019)	Björklund et al. (2021)	This work
RT code	POWR	FASTWIND	FASTWIND	CMFGEN
Hydro method	···	HYDWIND	···	Lambert *W*-function
$T_{\rm eff}$ [kK]	40.7	40	40.7	41
$\log g$	3.63	3.64	3.65	3.6
$R_*/R_\odot$	15.9	18.7	18.91	17.9
υ_∞ [km s^{-1}]	2046	2700	2302	2740
$\dot{M}$ [$10^{-6} M_\odot$ yr^{-1}]	1.6	5.2	2.5	2.7
f_∞ [$1/D_\infty$]	0.1	0.2	···	0.10

Note. These three models assume the same abundances as Bouret et al. (2012). The radiative transfer code used to perform the respective synthetic spectra is also marked, together with the code/methodology used to calculate the hydrodynamics. Equivalence between filling factor and clumping factor D_∞ (used by POWR) was made assuming the interclump medium is void, following Sundqvist & Puls (2018). Additionally, we include from the grid of Björklund et al. (2021), the closest parameters to ζ Puppis.

The Lambert-W procedure

ζ Puppis visual wavelength range

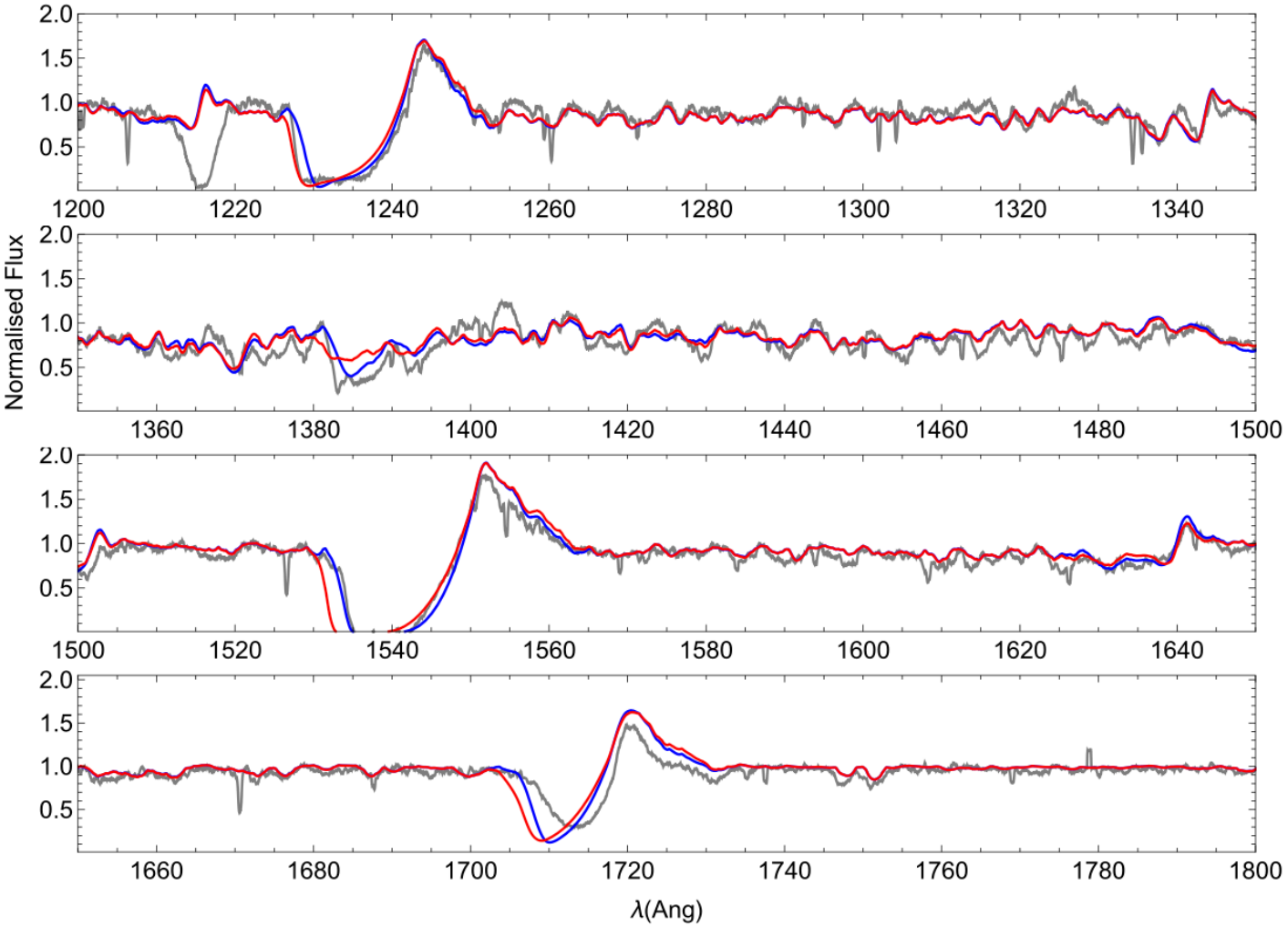

The Lambert-W procedure

ζ Puppis UV wavelength range

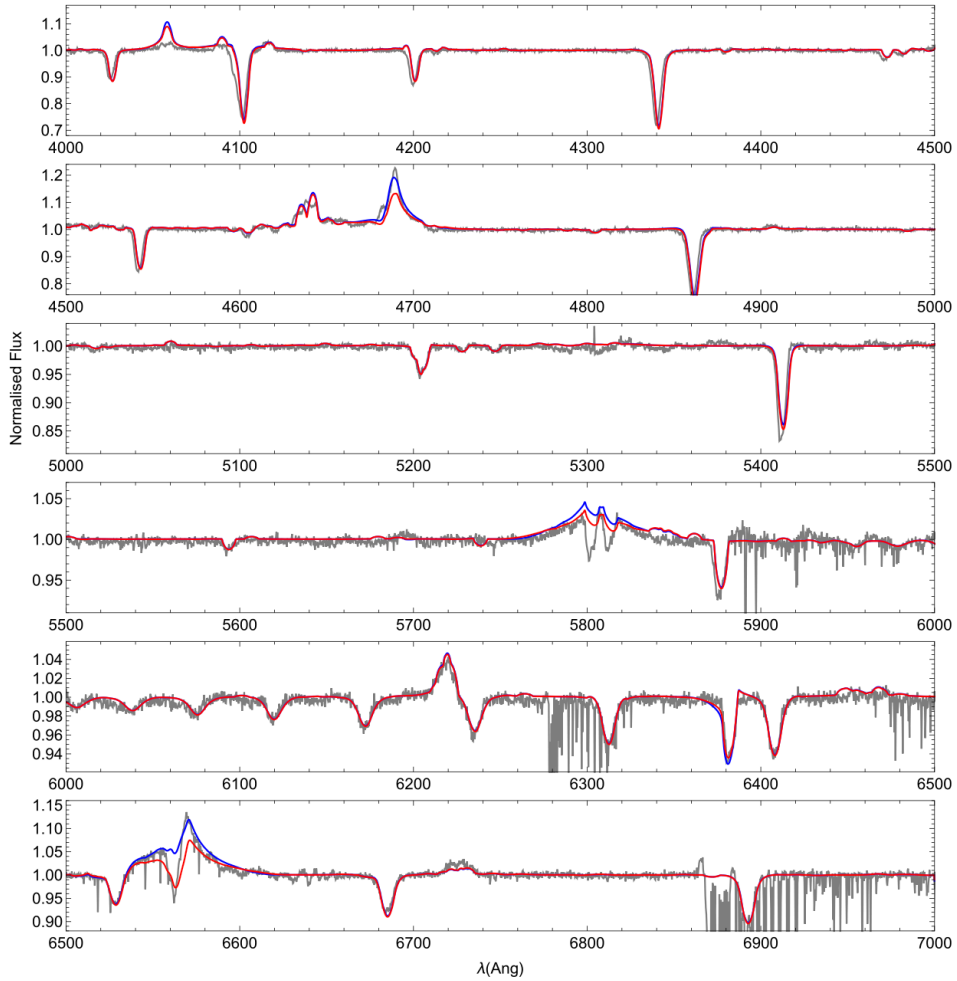

Figure 24. Comparison of the Lambert solution for ζ Puppis (red), compared with the initial CMFGEN spectrum (blue), with the observed FEROS spectrum for the visible range from 4000 to 7000 Å. These spectra were computed using CMF_FLUX (Busche & Hillier 2005), and rotational broadening was taken into account using standard convolution procedures. However, the H_α profile (and particularly the absorption component), for example, is modified when rotational broadening is explicitly calculated using a formal solution of the transfer equation (Hillier et al. 2012).

Self-consistent winds

LOCUS: Line fOrCe mUltiplier parameterS

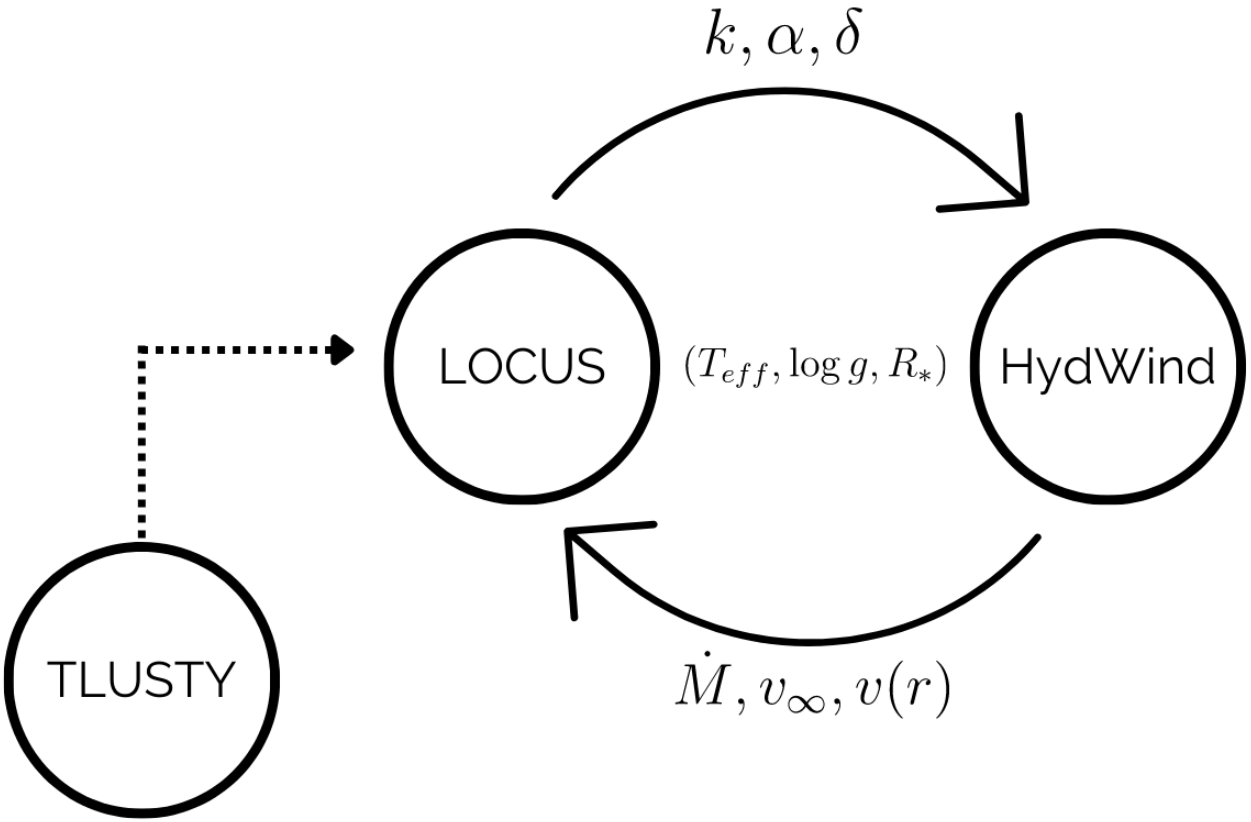

New Mass-loss rates

Grid Name	Elements
H	Hydrogen
HHe	Hydrogen Helium
CNO	Hydrogen Helium Carbon Nitrogen Oxygen

Parameter	Range	Step
$T_{\rm eff}$	$30000 - 50000$ [K]	1000 [K]
$\log g$	$2.8 - 4.3$ [dex]	0.1 [dex]
R_*	$7 - 70$ $[R_\odot]$	1.5 $[R_\odot]$

Grid	Initial Models	Converged Models	Filtered Models
H	9374	6009	911
HHe	9718	6121	913
CNO	8557	4004	617

New Mass-loss rates

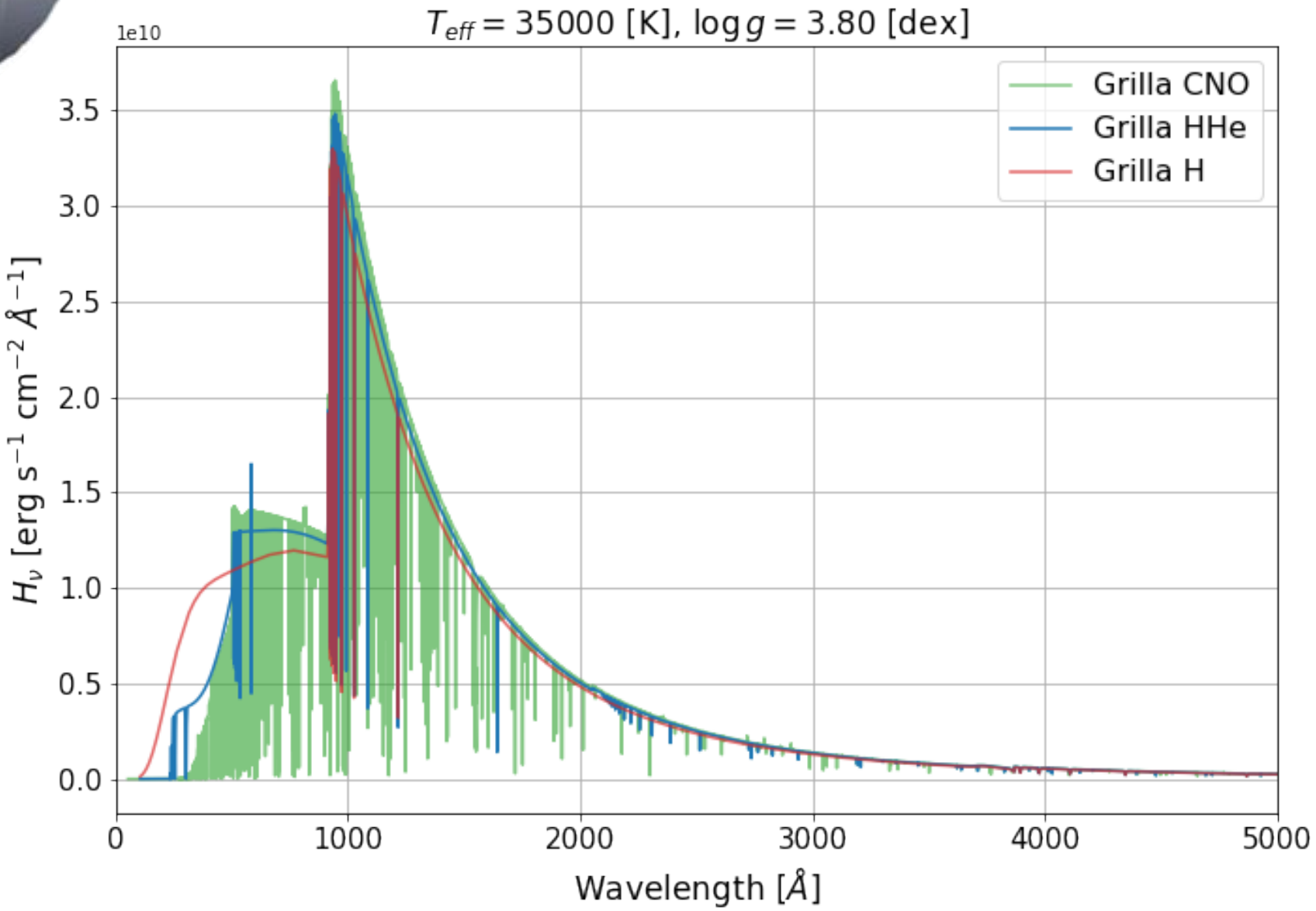

New Mass-loss rates

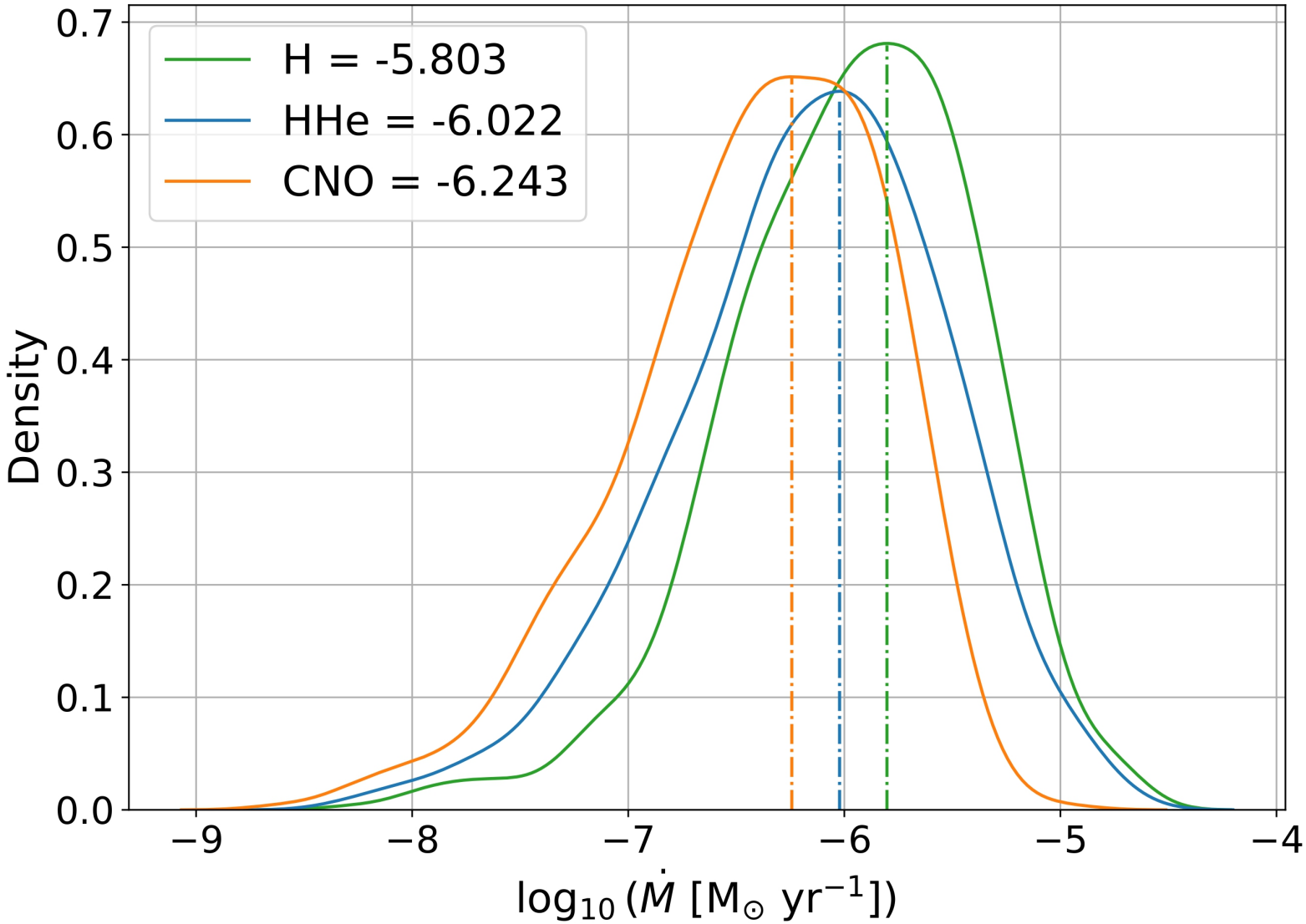

Michel Curé
Universidad de Valparaíso

New Mass-loss rates

$$\log \dot{M} = A \cdot \log\left(\frac{T_{\rm eff}}{1000\ {\rm K}}\right) + B \cdot \log g + C \cdot \log\left(\frac{R_*}{R_\odot}\right) + D$$

Grid	A	B	C	D	R^2
H	8.86 (±0.09)	-1.66 (±0.05)	1.82 (±0.05)	-16.2 (±0.09)	0.9486
HHe	12.6 (±0.17)	-2.23 (±0.05)	1.75 (±0.04)	-20.3 (±0.18)	0.9734
CNO	13.2 (±0.25)	-2.25 (±0.07)	1.78 (±0.05)	-21.3 (±0.24)	0.8893

New Mass-loss rates

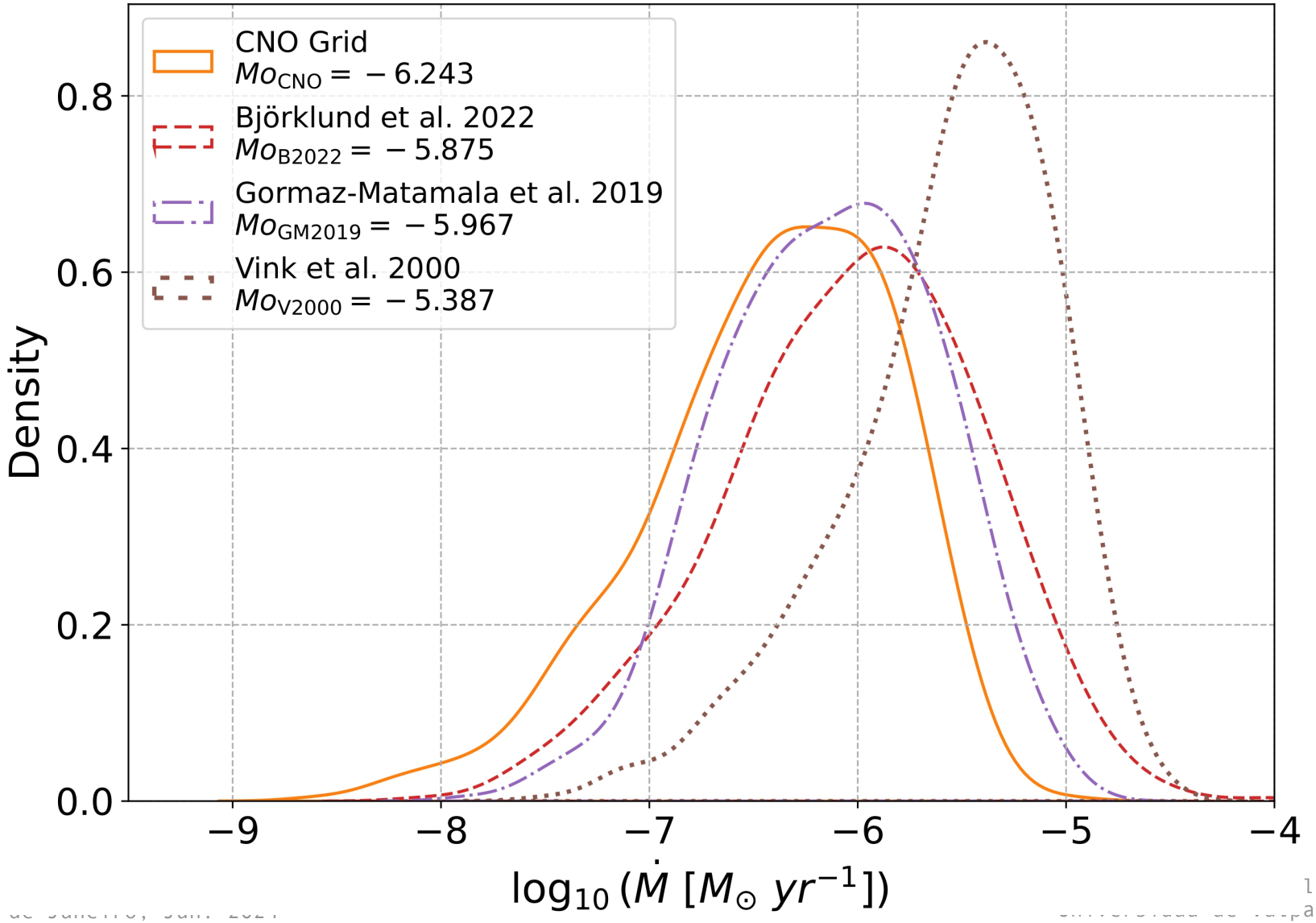

Quantitative Spectroscopy

requires

Plasma Physics,plasma is "normal" state of atmospheres and interstellar matter (plasma diagnostics, line broadening, influence of magnetic fields,...)
Atomic physics/Quantum mechanics,interaction light/matter (micro quantities)
Radiative transfer, interaction light/matter (macroscopic description)
Thermodynamics,thermodynamic equilibria: TE, LTE (local), NLTE (non-local)
Hydrodynamics,atmospheric structure, velocity fields, shockwaves,…
Machine Learning and Big Data

provides

Stellar properties, mass, radius, luminosity, energy production, chemical composition, properties of outflows
Properties of (inter) stellar plasmas, temperature, density, excitation, chemical comp., magnetic fields

Input for stellar, galactic and cosmological evolution and for stellar and galactic structure.

Massive stars binaries → Gravitational Waves

Conclusions

Slow wind solutions may solve some of the problems from massive stars:

- Winds from B[e] Supergiants (outflowing disk)
- Winds from BA Supergiants (WML relationship)
- Time-dependent Calculations (bifurcation, oscillation, clumping, instabilities,…)
- 2D-calculations
- Observations (constraints to theory)
- Grids for different Metallicities
- Different Machine Learning Algorithms

F I N

por ahora (for now)….

Gracias